

# Theory of exciton-exciton correlation in nonlinear optical response

Th. Östreich and K. Schönhammer

*Institut für Theoretische Physik, Universität Göttingen, Bunsenstraße 9, D-37073 Göttingen,  
Federal Republic of Germany*

L. J. Sham

*Department of Physics, University of California San Diego, La Jolla, California 92093-0319  
(August 13, 2018)*

## Abstract

We present a systematic theory of Coulomb interaction effects in the nonlinear optical processes in semiconductors using a perturbation series in the exciting laser field. The third-order dynamical response consists of phase-space filling correction, mean-field exciton-exciton interaction, and two-exciton correlation effects expressed as a force-force correlation function. The theory provides a unified description of effects of bound and unbound biexcitons, including memory-effects beyond the Markovian approximation. In the degenerate four-wave-mixing experiments, correlation effects are shown leading to polarization mixing, ringing, etc. The strong interaction, nonperturbative theory of the correlation function is numerically evaluated for a one-dimensional model. Approximations for the correlation function are presented.

71.35.+z, 42.50.Md

## I. INTRODUCTION

Transient four-wave-mixing (FWM) experiments have proven to be a powerful tool in probing and understanding optical coherence in semiconductors [1–5]. Subpicosecond spectroscopy yields information on the very early stages of time development of the carrier dynamics and many-particle correlations.

The essential physical picture behind the dynamical evolution of optically excited electrons and holes can be understood in simple terms [1,4–8]. First, the ultrafast dynamics of the exciting laser field with frequency near the fundamental band gap of a semiconductor creates coherent electron-hole (eh) pairs. Secondly, the motion of the carriers, dominated by the Coulomb interaction among them, leads to an ultrafast electric polarization as a source of light which can be observed. The scattering of carriers by other carriers, by phonons, and by defects leads to polarization decay and loss of optical coherence [9].

The density-matrix equations of motion which described the dynamics of the microscopic polarization and particle distribution functions were established by a number of groups [10–14]. Within the mean-field approximation, results for the ultrafast dynamics of the electron-hole pairs agreed well with the extant experimental findings, for example, for the dynamical Stark effect of the excitons in semiconductors [15] in a wide range of semiconductor bulk and quantum well systems. With recent advances in ultrafast nonlinear optical spectroscopy and in fabrication of semiconductor heterostructures, the use of three-pulse FWM, polarization [16,17] and phase sensitive measurements of the nonlinear polarization [18], and non-degenerate transient FWM [19] has led to effects beyond the mean-field approximation for exciton interaction and beyond the Markovian approximation for dephasing. Effects such as the polarization-dependent response of the excitons [17,20] and signatures of bound biexcitons [21–23] lead to more refined theoretical investigations beyond the mean-field approximation [16,17,24–32].

Polarization-mixing in the nonlinear optical response is caused by excitation of two excitons of opposite spins which first occur in second order of the Coulomb interaction [27]. The mean-field description which treats the interaction between excitons to first order in the Coulomb interaction can account for neither the polarization mixing nor the formation of bound biexcitons. This point was clearly demonstrated by Combescot and Combescot [33] who had stressed the importance of bound and unbound biexciton states for the excitonic ac-Stark shift as well as polarization effects [34]. The formation of para-biexcitons with singlet spin-states for the electrons and holes is one aspect of polarization-mixing which is most likely to be dominant for near resonant excitations of the fundamental exciton states. Moreover, even in the absence of bound biexcitons, the correlation in the continuum of two-exciton scattering states is also important [20,30].

In studying the optical processes in semiconductor systems, while much can be learned from ensembles of non-interacting atomic transitions [35–37] interacting with the radiation field or interacting localized (dense) two-level systems [38], the strong interaction and close proximity of the electrons in semiconductors provides a distinct avenue for new physics. It is well known that many-body effects lead to a renormalization of the external field (local-field effects) as well as to a renormalization of the interband transition energies (self-energy effects), depending sensitively on the density and dynamics of the surrounding electron-hole pairs [39,40]. In the linear response regime, these effects assume quantitative importance

[41]. However, the nonlinear properties of semiconductors in the weak nonlinear regime and in the high-excitation regime constitute a challenging problem, where the electron interaction physics must be added to carrier non-equilibrium and physics of quantum optics.

In the low-density or weakly nonlinear regime, i.e., to third-order in the external field, the dynamics of the semiconductor for near resonant excitation of the fundamental exciton resonances can be formulated in terms of a set of effective dynamical equations for the exciton polarization with nonlinear exciton-exciton interaction and space filling effects, which have been derived from the semiconductor Bloch equations (SBE) [2,42,43]. These effective equations provide a useful and physical picture of the origin of the nonlinearities and the observed phenomena, for example in the theory of the four-wave-mixing [2], photon echo [44] or the Rabi-oscillations in semiconductors [45]. Being within a mean-field description, the effective equations can provide no more information than the full semiconductor Bloch equations in the mean-field approximation.

The inclusion of biexcitonic effects as well as the possibility of polarization-mixing was first discussed in terms of phenomenological few-level models [16,17,24] to explain the temporal dependence of the FWM-signal including oscillations as a beating phenomena between bound and unbound biexciton states. In more microscopic theories, it was first shown in the equation-of-motion method by Axt and Stahl [25] and later in a diagrammatic approach by Maialle and Sham [27] that the semiconductor Bloch equations form a closed set of equations for the density matrix elements for any given order of the external field, depending on the initial state, which is usually the vacuum state of the electron-hole pairs. The so-called dynamics-controlled truncation scheme [25] provides a starting point for a microscopic theory of the polarization effects and has been applied to up to fifth-order processes [23]. The inclusion of biexcitonic effects for actual applications is mostly treated in a restriction to bound-state contributions and a *single* two-exciton state contribution [29] or perturbation theory in the Coulomb interaction [27,28]. The solution for the third-order susceptibility is inextricably bound to the solution of the four-particle problem.

In this paper, we give a microscopic theory of exciton interaction effects in nonlinear optical processes based on the Coulomb interaction between electrons. The detailed account provides the derivation behind our results published earlier [30,46]. The theory recovers the established mean-field results in the literature and formulates the rest of the interaction effects, termed correlation, in a concise manner. Particularly striking is the resulting equation of motion for the third-order nonlinear optical response shown to be driven by a number of terms with clearly identified physical origins: (1) phase-space-filling corrections, which are due to the Pauli-blocking of electrons and holes, (2) exciton-exciton mean-field interaction, and (3) the correlation term which is expressed as a two-exciton force-force correlation function. The derivation of the general equations of motion for any given order of the external field is given in Sec. II in terms of the Hubbard operators, using a complete basis set of the  $N$  eh-pair states. The Axt-Stahl theorem [25] manifests itself as, for example, the Hilbert space of one and two electron-hole pairs being sufficient for the third-order nonlinear response of the semiconductor. Details of the commutation algebra are relegated to Appendix A. An alternative derivation in terms of the density matrix is not recorded here to keep the length of the paper within bounds. The part of dephasing which is due to the electron interaction effects is included in our correlation function and the rest of the dephasing due to other causes is treated phenomenologically.

The correlation function approach gives a unified description of all correlation effects. It naturally encompasses the recently observed polarization mixing and bound-state biexcitonic molecules. The exact two-exciton correlation treats these effects on the same footing as the two-exciton scattering states which will be shown to be equally important. It contains the exact spin-dependent Coulomb correlation among the four particles and determines the spectral weight of the biexciton states for the source-term of the nonlinear response. These properties can be demonstrated by a numerical example of a one-dimensional model system with the advantage of not making decoupling approximations of the correlation effects. (See Sec. III). Details of the model are described in Appendix B.

Section IV gives an example of the correlation effects on a nonlinear optical process: a three-pulse four-wave-mixing experiment. Extensive new results of the numerical evaluation of the simple model are qualitatively compared with experimental results. Exact numerical evaluation of the correlation function is confined to simple models. For more realistic models to the semiconductor systems, we need reasonable approximations. A number of these are investigated in section V, including a microscopic expression for the excitation induced dephasing [47] and a brief comparison with the Boltzmann corrections in the quantum-kinetic equations [48]. We conclude with a summary of our theory and with a brief outline of future applications in section VI.

## II. AN EQUATION OF MOTION FOR THE THIRD-ORDER RESPONSE

We take as the fundamental approximation that, in the absence of the light-matter interaction, the Hilbert space of the semiconductor model consists of disconnected subspaces, which can be labeled according to the number of electron-hole (eh) pairs in the many-particle states. Let  $|0\rangle$  denote the trivial ground state with no eh-pairs present with energy  $\omega_{0,0} = 0$ . The one eh-pair subspace is the exciton subspace with states  $|E_{n,\sigma}^{(1)}\rangle$  with the quantum number  $n$ , a polarization index  $\sigma$  and energy  $\omega_{1,n,\sigma}$ . Both bound and scattering states are included in  $n$ . The polarization index labels a specific transition which, if optically active, corresponds to the helicity of the light required to excite the eh-pair-states that form the exciton. For example, in Zincblende structures, four p-type valence band states with total angular momentum  $3/2$  are connected via an optical dipole transition to an s-type conduction band with spin degeneracy. Due to selection rules, the  $m = 3/2(m = -3/2)$  electrons in the heavy-hole band are coupled via an optical transition with  $- (+)$  polarized photons to the  $s = 1/2(s = -1/2)$  spin states in the conduction band. The  $m = 1/2(m = -1/2)$  electrons in the light-hole band are coupled via an optical transition with  $- (+)$  polarized photons to the  $s = -1/2(s = 1/2)$  spin states in the conduction band. The spin-orbit interaction usually splits off a valence-band with total angular-momentum  $1/2$  and is neglected throughout this investigation.

The next relevant subspace is the biexciton Hilbert space with a complete set  $|E_m^{(2)}\rangle$  of bound and unbound states. Here, we introduce a single index  $m$  to label the set of quantum numbers for the states with energy  $\omega_{2,m}$ . Even though not all the biexciton states are computed due to the many-body nature of the problem, we keep all the states as long as possible because occasions arise that the biexciton states as intermediate states can be re-summed by virtue of the completeness theorem, similar to the treatment of the ac-Stark shift [33]. Such a step would be lost in a common approximation which restricts from the

start to one or two biexciton states.

The use of the subspaces of different exciton numbers as disconnected is implicit in previous works [25,27]. The disconnectedness is an approximation because states with different exciton numbers can be connected by the Coulomb interaction. The most important consequence is the neglect of the electron-hole pair fluctuations which affects the ground state and the dielectric screening of the Coulomb interaction. In other words, we define the ground state of the semiconductor as a vacuum state with respect to the exciton annihilation

$$B_{n,\sigma}|0\rangle = 0, \quad (2.1)$$

which means that no electron-hole pairs are present in the semiconductor ground state. The dielectric screening is approximately accounted for by the static dielectric constant of the semiconductor.

We define a total  $\sigma$ -polarization connected to an optical transition, which can be of arbitrary helicity, depending on the electronic states involved,

$$P_\sigma = \mu_\sigma^* \sum_{\mathbf{k}} \psi_{\mathbf{k},\sigma} \quad (2.2)$$

where the operator  $\psi_{\mathbf{k},\sigma}^\dagger$  creates a zero total momentum eh-pair with electron wave-vector  $\mathbf{k}$ , hole wave-vector  $-\mathbf{k}$  and polarization index  $\sigma$  and  $\mu_\sigma$  is the dipole matrix element between the electron and hole states, assumed to be independent of  $\mathbf{k}$ . Completeness of the operators leads to an equivalent expression of the  $\sigma$ -polarization in terms of exciton creation operators:

$$P_\sigma = \mu_\sigma^* \sum_n \alpha_{n,\sigma} B_{n,\sigma}, \quad (2.3)$$

where

$$\alpha_{n,\sigma} = \sqrt{V} \Phi_{n,\sigma}(\mathbf{x} = 0), \quad (2.4)$$

in terms of the exciton wave function at zero relative distance. The operator

$$B_{n,\sigma} = \sum_{\mathbf{k}} \psi_{\mathbf{k},\sigma} \phi_{\mathbf{k},n,\sigma}^* \quad (2.5)$$

creates an exciton state  $B_{n,\sigma}^\dagger|0\rangle = |E_{n,\sigma}^{(1)}\rangle$  with zero total momentum, energy  $\omega_{1,n,\sigma}$  and relative wave function  $\phi_{\mathbf{k},n,\sigma}$  in terms of momentum  $\mathbf{k}$ . The combination of the electron band  $\lambda_1$  and the hole band  $\lambda_2$  determines the polarization index  $\sigma = \sigma(\lambda_1, \lambda_2)$ . The laser central frequency  $\omega_p$  is implicitly subtracted from the exciton energy when we transfer to the rotating frame. The biexciton energy  $\omega_{2,m}$  then contains a reduction  $-2\omega_p$ . Note that the factor  $\alpha_{n,\sigma}$  depends on the sample volume  $V$  of the system for *bound* exciton states and is nonzero only for exciton states with *s*-wave symmetry. We take care of this volume dependence and show clearly how the final result is indeed volume independent.

Using the Dirac notation, we introduce the following Hubbard operators

$$\hat{X}_{N,\alpha;M,\beta} = |E_{N,\alpha}\rangle \langle E_{M,\beta}| \quad (2.6)$$

which can be used, in combination with the completeness relation

$$\mathbf{1} \equiv \sum_{N,\alpha} \hat{X}_{N,\alpha;N,\alpha}, \quad (2.7)$$

to express the exciton operator as

$$B_{n,\sigma} = \hat{X}_{0;1,n,\sigma} + \sum_{N \geq 1, \alpha, \beta} \langle E_{N,\alpha} | B_{n,\sigma} | E_{N+1,\beta} \rangle \hat{X}_{N,\alpha;N+1,\beta}. \quad (2.8)$$

The interaction of the semiconductor with a classical external laser field with central frequency  $\omega_p$  and field-strength  $\mathbf{E}(t) = \sum_{\sigma} E_{\sigma}(t) e^{-i\omega_p t} \mathbf{e}_{\sigma} + c.c.$  is given in the usual rotating wave approximation [35] by

$$H_I = - \sum_{n,\sigma} \left( E_{n,\sigma}^*(t) B_{n,\sigma} + \text{h.c.} \right) \quad (2.9)$$

with

$$E_{n,\sigma}(t) = \mu_{\sigma} \alpha_{n,\sigma}^* E_{\sigma}(t) \quad (2.10)$$

For comparison with previous work [43], this expression is the time-dependent renormalized Rabi frequency of a given polarization  $\sigma$  and transition  $n$  ( $\hbar \equiv 1$ ). The Hamiltonian of the semiconductor, from the disconnectedness of the subspaces, is

$$H = \sum_{N,\alpha} \omega_{N,\alpha} \hat{X}_{N,\alpha;N,\alpha} \quad (2.11)$$

which is equivalent to a multi-band microscopic Hamiltonian in second quantization. From the form of the interaction  $H_I$  it follows that the expectation values  $\langle \hat{X}_{0;N,\alpha} \rangle_t$  can be expressed as a power series in the external field

$$\langle \hat{X}_{0;N,\alpha} \rangle_t = \sum_{m=0}^{m_0} X_{N,\alpha}^{(N+2m)}(t) + O(E^{N+2m_0+2}). \quad (2.12)$$

The expectation value of a zero to  $N$ -pair transition is at least of order  $N$  in the external field. This *theorem* has already been proven by Axt and Stahl [25]. An important relation can be derived by the identity for an arbitrary state  $|\phi(t)\rangle$

$$\begin{aligned} \langle \hat{X}_{N,\alpha;M,\beta} \rangle_t &= \langle \phi(t) | \hat{X}_{N,\alpha;M,\beta} | \phi(t) \rangle \\ &= \langle \phi(t) | E_{N,\alpha} \rangle \langle 0 | \phi(t) \rangle \langle \phi(t) | 0 \rangle \langle E_{M,\beta} | \phi(t) \rangle \langle \hat{X}_{0;0} \rangle_t^{-1}. \end{aligned}$$

With  $\hat{X}_0^{(0)}(t) = 1$  from the initial condition of the semiconductor in its ground state  $|0\rangle$ , we find for the general expectation values

$$\langle \hat{X}_{N,\alpha;M,\beta} \rangle_t = \langle \hat{X}_{0;N,\alpha} \rangle_t^* \langle \hat{X}_{0;M,\beta} \rangle_t \langle \hat{X}_{0;0} \rangle_t^{-1}. \quad (2.13)$$

In order to calculate the  $\sigma$ -polarization we consider the equation of motion for  $\langle B_{n,\sigma} \rangle_t$ . Using the Hubbard operators it reads

$$\begin{aligned} i \frac{\partial}{\partial t} \langle B_{n,\sigma} \rangle_t &= (\omega_{1,n,\sigma} - i\Gamma) \langle B_{n,\sigma} \rangle_t + \sum_{N \geq 1} \sum_{\alpha, \beta} c_{n,\sigma;\alpha,\beta}^{(N)} \langle \hat{X}_{N,\alpha;N+1,\beta} \rangle_t \\ &\quad - E_{n,\sigma}(t) + \sum_{N \geq 1} \sum_{\alpha, \beta} E_{n,\sigma;\alpha,\beta}^{(N)} \langle \hat{X}_{N,\alpha;N,\beta} \rangle_t \end{aligned} \quad (2.14)$$

with

$$c_{n,\sigma;\alpha,\beta}^{(N)} = (\omega_{N+1,\beta} - \omega_{N,\alpha} - \omega_{1,n,\sigma}) \langle E_{N,\alpha} | B_{n,\sigma} | E_{N+1,\beta} \rangle \quad (2.15)$$

$$E_{n,\sigma;\alpha,\beta}^{(N)} = \sum_{\mathbf{q}} \mu_{\sigma} E_{\sigma}(t) \phi_{\mathbf{q},n,\sigma}^* \langle E_{N,\alpha} | 1 - n_{1,\mathbf{q},\sigma} + n_{2,\mathbf{q},\sigma} | E_{N,\beta} \rangle. \quad (2.16)$$

We have introduced the dephasing due to degrees of freedom not included explicitly (e.g. phonons) in a phenomenological way with the effective parameter  $\Gamma$ . Using Eqs. (2.12) and (2.13) we see that Eq. (2.14) can be considered as a linear differential equation with a (trivial) first-order source and nontrivial source terms of third and higher order. In the following we restrict ourselves to the contributions up to *third* order. Then using Eqs. (2.12) and (2.13) we see that only  $X_{1,n,\sigma}^{(1)}$  and  $X_{2,\alpha}^{(2)}$  have to be determined. As  $X_{1,n,\sigma}^{(1)}(t)$  obeys Eq. (2.14) without the terms involving the summations one obtains

$$X_{1,n,\sigma}^{(1)}(t) = i \int_{-\infty}^t e^{-i(\omega_{1,n,\sigma} - i\Gamma)(t-t')} E_{n,\sigma}(t') dt'. \quad (2.17)$$

The equation of motion for  $X_{2,\beta}^{(2)}$  reads

$$\begin{aligned} i \frac{\partial}{\partial t} X_{2,\beta}^{(2)} &= (\omega_{2,\beta} - i\Gamma_{xx}) X_{2,\beta}^{(2)} \\ &\quad - \sum_{n',\sigma';n'',\sigma''} E_{n'',\sigma''}(t) \langle E_{2,\beta} | B_{n'',\sigma''}^{\dagger} | E_{1,n',\sigma'} \rangle X_{1,n',\sigma'}^{(1)} \end{aligned} \quad (2.18)$$

with the biexciton phenomenological dephasing constant  $\Gamma_{xx}$ . In order to write the second term on the rhs of Eq. (2.14) in a compact form we use the explicit result Eq. (2.18) for  $X_{2,\beta}^{(2)}(t)$  in order to perform the summation over the biexciton quantum numbers  $\beta$ .

$$\begin{aligned} X_{2,\beta}^{(2)}(t) &= i \sum_{n',\sigma';n'',\sigma''} \int_{-\infty}^t e^{-i(\omega_{2,\beta} - i\Gamma_{xx})(t-t')} \\ &\quad \times E_{n'',\sigma''}(t') \langle E_{2,\beta} | B_{n'',\sigma''}^{\dagger} | E_{1,n',\sigma'} \rangle X_{1,n',\sigma'}^{(1)}(t') \end{aligned} \quad (2.19)$$

Using the identity

$$\begin{aligned} &i \sum_{n',\sigma';n'',\sigma''} E_{n'',\sigma''}(t) X_{1,n',\sigma'}^{(1)}(t) e^{i(\omega_{1,n'',\sigma''} + \omega_{1,n',\sigma'} - 2i\Gamma)t} \\ &= \frac{1}{2} \partial_t \left( \sum_{n',\sigma';n'',\sigma''} X_{n'',\sigma''}^{(1)}(t) X_{1,n',\sigma'}^{(1)}(t) e^{i(\omega_{1,n'',\sigma''} + \omega_{1,n',\sigma'} - 2i\Gamma)t} \right) \end{aligned} \quad (2.20)$$

we obtain after a partial integration

$$\begin{aligned} &\sum_{\beta} c_{n,\sigma;\tilde{n},\tilde{\sigma},\beta}^{(1)} X_{2,\beta}^{(2)}(t) \\ &= \frac{1}{2} \sum_{n',\sigma';n'',\sigma''} \left\{ \langle E_{1,\tilde{n},\tilde{\sigma}} | B_{n,\sigma} (H - \omega_{1,n,\sigma} - \omega_{1,\tilde{n},\tilde{\sigma}}) B_{n'',\sigma''}^{\dagger} | E_{1,n',\sigma} \rangle \right. \end{aligned} \quad (2.21)$$

$$\begin{aligned}
& \times X_{1,n',\sigma'}^{(1)}(t) X_{1,n'',\sigma''}^{(1)}(t) \\
& - \sum_{\beta} \int_{-\infty}^t \partial_{t'} \left( \langle E_{1,\tilde{n},\tilde{\sigma}} | B_{n,\sigma} e^{-i(\omega_{2,\beta} - i\Gamma_{xx})(t-t')} | E_{2,\beta} \rangle \right. \\
& \times \langle E_{2,\beta} | (H - \omega_{1,n,\sigma} - \omega_{1,\tilde{n},\tilde{\sigma}}) B_{n'',\sigma''}^{\dagger} | E_{1,n',\sigma} \rangle e^{i(\omega_{1,n'',\sigma''} + \omega_{1,n',\sigma'} - 2i\Gamma)(t-t')} \\
& \left. \times X_{1,n',\sigma'}^{(1)}(t') X_{1,n'',\sigma''}^{(1)}(t') e^{-i(\omega_{1,n'',\sigma''} + \omega_{1,n',\sigma'} - 2i\Gamma)(t-t')} dt' \right).
\end{aligned}$$

We can also perform the  $\beta$ -summation in the second term on the rhs of Eq. (2.21). For the derivative, we use the following identity, which holds for  $[B_{\tilde{n},\tilde{\sigma}}, B_{n,\sigma}] = 0$  and  $H|0\rangle = 0$

$$\begin{aligned}
& \partial_{\tau} \left( \langle E_{1,\tilde{n},\tilde{\sigma}} | B_{n,\sigma} (H - \omega_{1,n,\sigma} - \omega_{1,\tilde{n},\tilde{\sigma}}) e^{-iH\tau} B_{n'',\sigma''}^{\dagger} | E_{1,n',\sigma} \rangle \right. \\
& \times e^{i(\omega_{1,n'',\sigma''} + \omega_{1,n',\sigma'})\tau} \Big) \\
& \equiv -i \langle 0 | D_{\tilde{n},\tilde{\sigma};n,\sigma}(\tau) D_{n',\sigma';n'',\sigma''}^{\dagger} | 0 \rangle e^{i(\omega_{1,n'',\sigma''} + \omega_{1,n',\sigma'})\tau}.
\end{aligned} \tag{2.22}$$

Here we have introduced the “force” operator

$$D_{\tilde{n},\tilde{\sigma};n,\sigma} = [B_{\tilde{n},\tilde{\sigma}}, [B_{n,\sigma}, H]] \tag{2.23}$$

and the usual time dependence in the Heisenberg picture is given by  $D(\tau) = e^{iH\tau} D e^{-iH\tau}$ . This allows to write Eq. (2.21) in a compact form defining a memory kernel

$$F_{\tilde{n},\tilde{\sigma};n,\sigma}^{n',\sigma';n'',\sigma''}(\tau) := \langle 0 | D_{\tilde{n},\tilde{\sigma};n,\sigma}(\tau) D_{n',\sigma';n'',\sigma''}^{\dagger} | 0 \rangle, \tag{2.24}$$

for the second term on the rhs of Eq. (2.21). The matrix element in the mean-field contribution (first term on the rhs of Eq. (2.21)) can also be simplified, which gives

$$\begin{aligned}
\langle E_{1,\tilde{n},\tilde{\sigma}} | B_{n,\sigma} (H - \omega_{1,n,\sigma} - \omega_{1,\tilde{n},\tilde{\sigma}}) &= \langle E_{1,\tilde{n},\tilde{\sigma}} | ([B_{n,\sigma}, H] - \omega_{1,n,\sigma}) \\
&= \langle 0 | D_{\tilde{n},\tilde{\sigma};n,\sigma}
\end{aligned} \tag{2.25}$$

and we finally arrive at

$$\begin{aligned}
\sum_{\beta} c_{n,\sigma;\tilde{n},\tilde{\sigma},\beta}^{(1)} X_{2,\beta}^{(2)}(t) &= \frac{1}{2} \sum_{n',\sigma',n'',\sigma''} \left\{ \langle 0 | D_{\tilde{n},\tilde{\sigma};n,\sigma} B_{n',\sigma'}^{\dagger} B_{n'',\sigma''}^{\dagger} | 0 \rangle \right. \\
&\times X_{1,n',\sigma'}^{(1)}(t) X_{1,n'',\sigma''}^{(1)}(t) \\
&- i \int_{-\infty}^t e^{-2\Gamma(t-t')} F_{\tilde{n},\tilde{\sigma};n,\sigma}^{n',\sigma';n'',\sigma''}(t-t') \\
&\left. \times X_{1,n',\sigma'}^{(1)}(t') X_{1,n'',\sigma''}^{(1)}(t') dt' \right\}.
\end{aligned} \tag{2.26}$$

Here it is necessary to assume the relation  $\Gamma_{xx} \equiv 2\Gamma$  to use the identity Eq. (2.22). The memory function in Eq. (2.24) is a four-point correlation function in terms of electron (hole) operators. As the operators  $A_{n,\sigma}(\mathbf{q})$  can be expressed in terms of *finite* center-of-mass

exciton operators  $B_{n,\sigma}(\mathbf{q})$ ,  $F(\tau)$  can be considered a two-exciton correlation function. From the double commutator definition of the  $D$  operators, Eq. (2.24) is a *force-force* correlation function [49]. An explicit form of the operator  $D$  is derived in Appendix A using a specific semiconductor model.

The first expression on the rhs of Eq. (2.26) describes the correlations between excitons as in the usual mean-field semiconductor Bloch equations (MFSBE) [11,2,43,44]. It is only nonzero for excitons with zero center-of-mass momentum and with *identical polarization*, i.e., each pair of charged carriers (electrons and holes) must belong to the same bands, and consequently does not produce polarization mixing. For comparison with previous work on the MFSBE and earlier work on exciton-exciton interaction [50–52], we introduce the matrix elements

$$\beta_{\tilde{n},\tilde{\sigma};n,\sigma}^{n',\sigma';n'',\sigma''} = \langle 0 | D_{\tilde{n},\tilde{\sigma};n,\sigma} B_{n',\sigma'}^\dagger B_{n'',\sigma''}^\dagger | 0 \rangle, \quad (2.27)$$

$$\gamma_{\tilde{n},\tilde{\sigma};n,\sigma}^{n',\sigma';n'',\sigma''} = \langle 0 | D_{\tilde{n},\tilde{\sigma};n,\sigma} D_{n',\sigma';n'',\sigma''}^\dagger | 0 \rangle. \quad (2.28)$$

As  $D_{\tilde{n},\tilde{\sigma};n,\sigma}(\tau)|0\rangle = 0$ , the correlation function  $F(\tau)$  can be written as a time-ordered product and standard Feynman diagrams can be used e.g. to set up approximation schemes. From a diagrammatic analysis to all orders the rigorous polarization selection rule  $\sigma + \tilde{\sigma} = \sigma' + \sigma''$  can easily be read off [27]. The fact that the third-order polarizability can be expressed in terms of this correlation function depending on a *single* time difference is due to the simplicity of the semiconductor ground state Eq. (2.1) approximated by the vacuum state of the bound and unbound excitons.

An additional contribution to the third-order nonlinear response is given by the phase-space filling factor, which is due to the Pauli blocking of electrons. This term is assumed to play a minor role in the low-density regime of optical excitations of semiconductors, but we include this contribution here to preserve the exactness of our expression to third order in the exciting field. Keeping the  $N = 1$  contribution in Eq. (2.16) we find with Eq. (2.13)

$$\begin{aligned} \sum_{\alpha,\beta} E_{n,\sigma;\alpha,\beta}^{(1)} \langle \hat{X}_{1,\alpha;1,\beta} \rangle_t &= \sum_{\tilde{n},\tilde{\sigma},n',\sigma',n'',\sigma''} C_{\tilde{n},\tilde{\sigma};n,\sigma}^{n',\sigma';n'',\sigma''} E_{n',\sigma'}(t) \\ &\times \left( X_{1,\tilde{n},\tilde{\sigma}}^{(1)}(t) \right)^* X_{1,n'',\sigma''}^{(1)}(t) \end{aligned} \quad (2.29)$$

The phase-space-filling parameter depends on the explicit exciton wave-functions, c.f. Appendix A:

$$\begin{aligned} C_{\tilde{n},\tilde{\sigma};n,\sigma}^{n',\sigma';n'',\sigma''} &= \delta_{\sigma,\sigma'} \alpha_{n',\sigma'} \sum_{\mathbf{q}} \phi_{\mathbf{q},n,\sigma}^* \\ &\times \langle E_{1,\tilde{n},\tilde{\sigma}} | 1 - n_{1,\mathbf{q},\sigma} + n_{2,\mathbf{q},\sigma} | E_{1,n'',\sigma''} \rangle. \end{aligned} \quad (2.30)$$

The exact third-order nonlinear polarization  $P_{n,\sigma}^{(3)}(t)$  is given by the solution of the following linear differential-equation with a complete set of source terms

$$\begin{aligned} \left( \frac{\partial}{\partial t} + i\omega_{1,n,\sigma} + \Gamma \right) P_{n,\sigma}^{(3)}(t) &= -i \sum_{\tilde{n},\tilde{\sigma},n',\sigma',n'',\sigma''} \left( X_{1,\tilde{n},\tilde{\sigma}}^{(1)}(t) \right)^* \\ &\left\{ C_{\tilde{n},\tilde{\sigma};n,\sigma}^{n',\sigma';n'',\sigma''} E_{n',\sigma'}(t) X_{1,n'',\sigma''}^{(1)}(t) + \frac{1}{2} \beta_{\tilde{n},\tilde{\sigma};n,\sigma}^{n',\sigma';n'',\sigma''} X_{1,n',\sigma'}^{(1)}(t) X_{1,n'',\sigma''}^{(1)}(t) \right. \\ &\left. - \frac{i}{2} \int_{-\infty}^t e^{-2\Gamma(t-t')} F_{\tilde{n},\tilde{\sigma};n,\sigma}^{n',\sigma';n'',\sigma''}(t-t') X_{1,n',\sigma'}^{(1)}(t') X_{1,n'',\sigma''}^{(1)}(t') dt' \right\}. \end{aligned} \quad (2.31)$$

This equation expresses succinctly the physical origins of the source terms which drive the third-order polarization: the first term in the curly bracket being the phase-space filling, the second the Hartree-Fock or mean-field terms (of first order in the Coulomb interaction between excitons), and the last the biexciton correlation. The source terms require a solution of the linear-response problem of Eq. (2.17). The above derivation of the third-order nonlinear response can be extended to higher order in the external field. However, the higher-order correlation functions involved no longer have the simple structure of the third-order response force-force correlation function.

### III. EXCITON-EXCITON CORRELATIONS

The correlation function formulation of the last section provides us with a powerful framework to compute the correlation effects of the two excitons based on treating the interaction among the two electrons and two holes on an equal basis. In this section, we start with the nonlinear optical processes which lead to the excitation of the excitons and discuss some general properties inferred from a study of a one-dimensional system, where the correlation function can be calculated numerically for relatively large system sizes without approximating the effects of the many-body interaction. We calculate the spectral-function for the 1s-exciton contribution to the third-order optical response for a one-dimensional semiconductor model. This is done in the frequency representation with the use of the Lanczos algorithm [53]. The details of the one-dimensional semiconductor model in real-space are defined in Appendix B.

The selection rule which connects the helicity of the exciting light to the spins of the electron and hole gives rise to different types of two-exciton excitations depending on the energy level structures. For a semiconductor with Zincblende structure, where spin-orbit leads to a four-fold degenerate valence-band maximum, Fig. 1 illustrates the three types:

*Type-I* In heterostructures, the strain or confinement can lead to a considerable heavy- and light-hole splitting  $\Delta_{hl-lh}$ . This allows for a selective excitation of heavy- or light-hole exciton states.

*Type-II* In bulk systems, circularly polarized light excites a combination of heavy- and light-hole excitons simultaneously.

*Type-III* Polarization mixing can be induced by a linearly polarized light. A special situation arises, when conduction band states are common for both excited exciton species, in contrast to the type-II excitation. A three-pulse four-wave-mixing geometry can distinguish this analog of the  $\Lambda$ -transition in quantum optics from the decoupled transitions.

Correlation among the electrons and holes depends sensitively on their angular momenta (spins) and, in turn, influences the polarization dependence in the nonlinear optical response. We sort out for each combination of spins the possible types of excitations listed above:

- *Opposite-spin excitons:*

If the two excitonic transitions belong to different conduction and valence bands, i.e., no single-particle states are the same, e.g., the polarization mixing of simultaneous

excitations of the  $m = -3/2$  valence band to conduction-band  $s = -1/2$  transition with a *positive* circular polarization of the light-field and the  $m = 3/2$  valence band to conduction-band  $s = 1/2$  states with a *negative* circular polarization of the light-field respectively, this excitation condition is type-I. In the absence of a significant band-splitting, e.g., in bulk systems, a *positive* circular excitation will excite light-hole excitons from valence band  $m = -1/2$  to conduction-band  $s = 1/2$  states as well as from valence band  $m = -3/2$  to conduction-band  $s = -1/2$ . This situation belongs to the type-II excitation. Although both excitons have equal-spin, the exciton energies and transition strengths are different and can be distinguished. In both cases above, (one type-I and one type-II), the hole *and* the electron states belong to different bands. The correlation among the four charged carriers is now entirely determined by Coulomb effects since no Pauli-blocking is encountered in the band.

- *Parallel-spin excitons:*

When the two exciton transitions have common hole and electron bands, their spins are parallel. For a type-I excitation, with only, say, positive circularly polarized excitation, only spin +1-excitons are populated. A three-pulse experiment can distinguish between the equal-spin and the opposite-spin correlations in the response signal. This point is discussed in the context of the four-wave-mixing experiments in the next section. The most prominent feature of the equal-spin correlation is the absence of a bound biexcitonic molecule. This shows up clearly in the one-dimensional model. A type-II excitation will mix the opposite- and parallel-spin correlations and the analysis of the FWM geometry is more complicated, due to the natural interference of the individual contributions.

- *Coupled-spin excitons:*

The type-III excitation arises when either the electron or hole states but not both share a common band. For example, linear excitation of heavy- and light-hole excitons in *GaAs* will induce transitions from the  $m = -3/2$  valence states with photons of positive helicity as well as transitions from the  $m = 1/2$  valence states with photons of negative helicity to common conduction-band states with  $s = -1/2$ . The corresponding correlation function is similar to the parallel-spin case in the sense that the conduction-band electrons are subject to the Pauli exclusion. With a finite heavy/light hole splitting, this type-III excitation is sensitive to the time delay between the two exciting pulses in a three-pulse FWM experiment and can, thus, be distinguished from the parallel-spin type-I case.

Fig. 2 shows the correlation function spectrum for the diagonal 1s-exciton contribution calculated in a one-dimensional semiconductor model. The opposite-spin case (solid line) and the parallel-spin case (dashed line) are shown. The zero of energy corresponds to the energy of two non-interacting 1s-excitons, which is spin independent. Resonances at negative energies  $\omega$  correspond to *bound* excitonic molecules (biexcitons). In this case, the binding energy of the biexciton is approximately 1.5 meV. In Fig. 2 (a), the masses of electrons and hole are identical (positronium-limit). The bound-state of the para-biexciton is the most significant feature at low energies, since the binding energy is expected to be much smaller than the usual excitonic binding energies, which is 10 meV in this model for the 1s-state.

The parallel-spin case has more pronounced spectral weight at lower positive energies, but a bound-state is not expected to exist. The spectra have a maxima at higher energies before dropping to zero. The bandwidth of a single-electron band is 50 meV. It is surprising that the spectrum is almost zero above the free electron-hole pair-state bandwidth of 100 meV. However, a high energy-resonance is visible.

This distant resonance moves to lower energies in Fig. 2 (b), when the ratio of the electron-to-hole mass is reduced to  $m_e/m_h = 0.15$ , found in semiconductors like in *GaAs*. The reduced mass of electrons and holes is kept constant. More spectral features appear in the lower energy regime. In principle, more bound-states should appear for negative energies. A dip-like structure can be found at almost the same position for the opposite-spin and parallel-spin case. In the case of opposite-spin correlations, we find increased spectral weight for smaller positive energies. This can be easily understood, if one eh-pair is in the  $1s$ -exciton state, whereas the second eh-pair is quasi-free (dissociated).

This can be seen in Fig. 2 (c) for infinite hole mass (molecular limit). The opposite-spin case has pronounced spectral features at low energies. More resonances appear, if the spectral broadening is decreased. The resonances can be classified as (1) bound excitonic molecules at negative energies, which simply are the ground-states of two electrons in a static potential of two *heavy* holes with varying distance, and (2) scattering resonances, which are anti-binding states with molecular character. These anti-binding states do contribute to the nonlinear optical response. For example, the first large resonance at positive energies results from the configuration where the two holes are extremely close together. This is similar to the configuration of a helium atom from the view of the fast moving electrons. The spectral weight of the force-force correlation function favors states with small distance of the charged carriers, as can be seen from the real-space representation of the state  $D^\dagger|0\rangle$  in Eq. (B13). A third resonance is clearly visible at the same energy position for both spin cases at  $\omega \approx 10$  meV. This resonance is the largest feature in the case of parallel-spin excitons. The analysis of small systems of up to 10-sites strongly suggests that this feature originates from Coulomb correlation of electrons and holes in the anti-bonding state, where the holes are located on neighboring sites. This explains the feature in both spectra. The position of the resonance is only weakly dependent on the on-site Coulomb interaction. We have verified that the spectral resonance from a state with a single  $1s$ -exciton and a dissociated eh-pair gives much a smaller contribution at this energy. The dip for parallel-spin excitons in Fig. 2 (c) goes almost to zero and separates a small band of biexciton scattering states with weakly repulsive interacting pairs of  $1s$ -excitons from the anti-bonding resonance. For opposite-spin excitons, a spectral hole emerges at zero energy. Spectral weight from the product state of two  $1s$ -excitons with zero center-of-mass momentum is recovered in the mean-field contribution to the nonlinear optical response.

The force-force correlation spectrum has a large number of spectral features at the exact biexciton energies, which include bound-state as well as scattering-state contributions. The correlation function approach treats these states on an equal footing. We expect a similar behavior also for more realistic  $2d$ - or  $3d$ -models.

#### IV. APPLICATION TO FOUR-WAVE-MIXING

In this section, we investigate the correlation effects in four-wave-mixing (FWM) experiments with semiconductor heterostructures in the low-density excitation regime where the third-order theory in the exciting field is valid. Polarization mixing of electrons and holes with different spin can be induced and probed using cross-polarized laser excitation. With the proliferation of new experiments which aim at probing correlations, we use, as illustrations of application of our theory, two specific experimental situations with the simple type-I excitation. The first paradigm experiment [20], by resonantly exciting excitons in quantum-well structures, clearly demonstrates the signature of polarization-mixing in these systems for the ultrafast nonlinear response, even in the absence of biexcitonic molecules. The actual numerical simulations are performed with the quasi one-dimensional semiconductor correlation function (Sec. 3) to model the spin-dependent effects and are not intended to quantitatively describe the experiment. As a second example, we study the effects of bound and unbound two-exciton states and discuss the “beating” phenomena of the biexciton resonance for type-I excitations, which was identified as quantum-beats [22] between bound and unbound biexciton states and which our calculation shows to be a *ringing* of the bound-state resonance alone.

The typical experimental setup is sketched in Fig. 3 for a three-pulse four-wave-mixing geometry. This experiment leads to polarization mixing when pulses (2) and (3) have opposite helicity. In this case, equal populations of excitons with opposite angular momenta are excited for type-I excitation. In the mean-field description, no third-order polarization  $P^{(3)}(\mathbf{k}_f)$  exists to diffract probe pulse (1) in the  $\mathbf{k}_f = \mathbf{k}_3 + \mathbf{k}_2 - \mathbf{k}_1$  direction for any time delay  $T$ . However, beyond the mean-field theory, correlation effects between opposite-spin excitons cause polarization mixing.

To allow for an analytical discussion, we consider the limit of ultrashort light pulses with identical central frequency, which simplifies most of the following calculations. In this case, the exciting laser field is given by

$$\mathbf{E}(t) = \sum_j \mathbf{E}(\mathbf{k}_j) \delta(t + \tau_j). \quad (4.1)$$

We emphasize that a delta-pulse approximation is used only in the time integration and not in the frequency integration since it gives a infinite broad spectral width. The laser pulse in the propagation direction  $\mathbf{k}_j$  interacts with the sample at time  $t = -\tau_j$ . The corresponding *area* of the light pulse is given by  $\mathbf{E}(\mathbf{k}_j)$ . The summation index  $j$  labels the different pulses involved the multi-wave experiment. The first-order polarization of a single exciton transition is easily calculated from Eq. (2.17)

$$X_{n,\sigma}^{(1)}(t) = i\mu_\sigma \alpha_{n,\sigma}^* \sum_j e^{-i(\omega_{n,\sigma} - i\Gamma_\sigma)(t + \tau_j)} \Theta(t + \tau_j) E_\sigma(\mathbf{k}_j). \quad (4.2)$$

Here,  $E_\sigma(\mathbf{k}_j) = \mathbf{E}(\mathbf{k}_j) \cdot \mathbf{e}_\sigma$  is the projection of the laser field in the propagation direction  $\mathbf{k}_j$  onto the polarization unit-vector  $\mathbf{e}_\sigma$  of the  $(n, \sigma)$  transition. The dephasing  $\Gamma_\sigma$  may depend on the polarization of the transition. In the exciton picture, the total nonlinear polarization to third-order in the external fields is given by Eq. (2.31). The contribution from the phase-space-filling, well documented in the literature [54,2,39], plays only a minor

role in the low-density limit. We focus on the remaining contribution from the mean-field part and the genuine correlation which can be treated on equal footing. Correlation lead to the following nonlinear complex polarization for the transition  $(n, \sigma)$

$$P_{n,\sigma}^{(3)}(t) = -\frac{i}{2}\mu_{\sigma}^* \alpha_{n,\sigma} e^{-i(\omega_{n,\sigma} - i\Gamma_{\sigma})t} \sum_{\substack{\bar{n}, \bar{\sigma}, n', \sigma', n'', \sigma'' \\ j_1, j_2, j_3}} (\alpha \mathcal{E} \phi) \quad (4.3)$$

$$\{ \Theta(t + \tau_{j_1}) \Theta_{21} \Theta_{32} C_{12}(t) + \Theta(t + \tau_{j_2}) \Theta_{12} \Theta_{32} C_{22}(t) \\ + \Theta(t + \tau_{j_1}) \Theta_{31} \Theta_{23} C_{13}(t) + \Theta(t + \tau_{j_3}) \Theta_{13} \Theta_{32} C_{33}(t) \}.$$

with  $\Theta_{kl} = \Theta(\tau_k - \tau_l)$  and an exciton wave-function dependent factor

$$\alpha \equiv \alpha_{\bar{n}, \bar{\sigma}} \alpha_{n', \sigma'}^* \alpha_{n'', \sigma''}^*, \quad (4.4)$$

with  $\alpha_{n,\sigma}$  defined in Eq. (2.4). The exciton-label dependence of  $\alpha$  on the left is understood. The external field and helicity dependence is contained in the factor

$$\mathcal{E} \equiv \mu_{\bar{\sigma}} E_{\bar{\sigma}}^*(\mathbf{k}_{j_1}) \mu_{\sigma'} E_{\sigma'}(\mathbf{k}_{j_2}) \mu_{\sigma''} E_{\sigma''}(\mathbf{k}_{j_3}). \quad (4.5)$$

A general phase  $\phi$  is due to the delay between the short pulses

$$\phi \equiv e^{i(\omega_{\bar{n}, \bar{\sigma}} + i\Gamma_{\bar{\sigma}})\tau_{j_1}} e^{-i(\omega_{n', \sigma'} - i\Gamma_{\sigma'})\tau_{j_2}} e^{-i(\omega_{n'', \sigma''} - i\Gamma_{\sigma''})\tau_{j_3}}. \quad (4.6)$$

The nontrivial part of the polarization dynamics is contained in the time-dependent function ( $t > -\tau_a, \tau_a < \tau_b$ )

$$C_{a,b}(t) = \int_{-\tau_a}^t e^{i(\omega_{n,\sigma} + \omega_{\bar{n}, \bar{\sigma}} - \omega_{n', \sigma'} - \omega_{n'', \sigma''})t'} e^{-(\Gamma_{\sigma'} + \Gamma_{\sigma''})t'} \int_0^{t' + \tau_b} \tilde{F}(\tau) d\tau dt'. \quad (4.7)$$

Eq. (4.7) contains the complete Coulomb correlation beyond the mean-field approximation. The integral kernel is the memory function, which can be calculated with the knowledge of the exciton-exciton correlation function,

$$F_{\bar{n}, \bar{\sigma}; n, \sigma}^{n', \sigma'; n'', \sigma''}(\tau) = e^{-i(\omega_{n', \sigma'} + \omega_{n'', \sigma''})\tau} \tilde{F}(\tau). \quad (4.8)$$

For the numerical calculation, we always use the resonant condition for the temporal evolution of  $\tilde{F}(\tau)$  in Eq. (4.8), i.e.  $\omega_{n'} + \omega_{n''} = 0$ . For non-resonant excitation, the detuning-dependent integrand in Eq. (4.7) has no phase dependence for the *diagonal* contributions of the correlation function.

We now consider the response from the non-degenerate exciton ground-states (1s) only, with near-resonant excitation of the central laser frequency, i.e.  $\omega_{n=1s, \sigma} = \omega_{\sigma}$ , and neglect the transition label  $n = 1s$ . We also set  $\Gamma_{\sigma} = \Gamma$  for convenience. This simplifies the general expression Eq. (4.3) and Eq. (4.7) considerably:

$$C_{a,b}(t) = \int_{-\tau_a}^t e^{-2\Gamma t'} \int_0^{t' + \tau_b} \tilde{F}(\tau) d\tau \quad (t > -\tau_a, \tau_a < \tau_b). \quad (4.9)$$

The simplest experiment which is able to distinguish equal-spin from opposite-spin correlation is the three-beam experiment of Fig. 3, where the two pulses (2) and (3) interact

with the sample at the same time. Assuming that lasers (2) and (3) interact with the sample at  $\tau_2 = \tau_3 = 0$  we define the delay time  $\tau_1 = T$ . The correlation function is now diagonal with respect to the exciton indices and has the spectral representation with  $f_m = \langle 0|D|E_m\rangle$

$$\tilde{F}(\tau) = \sum_m |f_m|^2 e^{-i\omega_m \tau} \quad (4.10)$$

where the  $m$ -summation includes all contributions from bound ( $\omega_m < 0$ ) and unbound ( $\omega_m > 0$ ) biexciton states  $|E_m\rangle$  and the implicit transition indices are understood. We find for Eq. (4.9) with  $\tau_a = T$ ,  $\tau_b = 0$  for negative time delay  $T < 0$  and  $t > -T$ ,

$$\begin{aligned} \tilde{C}(t, T) &:= \sum_m \int_{-T}^t e^{-2\Gamma t'} \int_0^{t'} |f_m|^2 e^{-i\omega_m \tau} \\ &= \sum_m |f_m|^2 \left\{ \frac{e^{-(2\Gamma+i\omega_m)t} - e^{(2\Gamma+i\omega_m)T}}{i\omega_m(i\omega_m + 2\Gamma)} - \frac{e^{-2\Gamma t} - e^{2\Gamma T}}{i\omega_m 2\Gamma} \right\}. \end{aligned} \quad (4.11)$$

The second term of Eq. (4.11) is simplified by a sum rule

$$\sum_m |f_m|^2 \omega_m^{-1} = \beta, \quad (4.12)$$

which can easily be derived from the usual Lehmann representation of the correlation function and using Eq.(2.27). The parameter  $\beta$  is the mean-field exciton-exciton interaction parameter with four identical exciton indices (1s). For the parallel-polarized case, this contribution is canceled exactly by the explicit mean-field contribution to the third-order nonlinear polarization. This can be seen by inspection of the second and third terms on the rhs of Eq. (2.31), when we set  $F(\tau) \equiv i\beta\delta(\tau)$ . For opposite-spin excitation, this parameter  $\beta$  is zero. In the following we define  $C(t, T)$  to be the result of Eq. (4.11) after the cancellation:

$$C(t, T) := \sum_m |f_m|^2 e^{(2\Gamma+i\omega_m)T} \left\{ \frac{e^{-(2\Gamma+i\omega_m)(t+T)} - 1}{i\omega_m(i\omega_m + 2\Gamma)} \right\} \quad (4.13)$$

and, for comparison, the mean-field part

$$C_{MF}(t, T) := -i\beta e^{2\Gamma T} \left\{ \frac{e^{-2\Gamma(t+T)} - 1}{2\Gamma} \right\}. \quad (4.14)$$

The sum-rule Eq. (4.12) does not imply that the mean-field instantaneous contribution in the nonlinear response has completely disappeared in Eq. (4.13). Mean-field and correlation contributions are treated here on an equal footing as part of the Coulomb interaction of the charged carriers. In the response function Eq. (4.12), the mean-field contribution is recovered in the *large* dephasing limit, i.e.,  $\Gamma \gg \omega_x$ . In the following, we assume equal field strength for all pulses with real amplitude  $E_\sigma$ . We evaluate the signal according to the following general rules:

1. *Spatial dependence.*

The external sources, Eq. (4.5), for the nonlinear polarization Eq. (4.3) have to be selected with the correct spatial phase dependence. For the signal in  $\mathbf{k}_f$ -direction, the index combinations  $\mathbf{k}_{j_2} = \mathbf{k}_2, \mathbf{k}_{j_3} = \mathbf{k}_3$  and  $\mathbf{k}_{j_2} = \mathbf{k}_3, \mathbf{k}_{j_3} = \mathbf{k}_2$  are possible with  $\mathbf{k}_{j_1} = \mathbf{k}_1$  fixed.

## 2. Time dependence.

The set  $\{j_1, j_2, j_3\}$  determines the type of response term  $C_{ij}$  and the corresponding  $\Theta$ -functions. This will determine the temporal details of the signal, depending on the time-order of the incoming pulses.

## 3. Helicity dependence.

The polarization of the transitions and the helicity of the exciting fields determine the correct type of correlation function and field amplitude projection  $E_\sigma$ .

## 4. Transition dependence.

Perform the summation over the exciton quantum numbers after the polarization dependence is determined in the above steps. Symmetry arguments can be used to reduce the actual number of terms.

Applying rules (1) and (2) in the case of a near-resonant excitation of the heavy-hole/light-hole  $1s$ -excitons, we find for the time-resolved nonlinear polarization, using  $\mu_\sigma \equiv \alpha_{n=1s,\sigma}^* \mu_\sigma$

$$P_\sigma^{(3)}(t) = -\frac{i}{2} \mu_\sigma^* \sum_{\sigma', \bar{\sigma}, \sigma''} e^{-i(\omega_\sigma - i\Gamma)t} e^{i(\omega_{\bar{\sigma}} + i\Gamma)T} \mu_{\bar{\sigma}}^* E_{\bar{\sigma}}^*(\mathbf{k}_1) \times \left( \mu_{\sigma'} E_{\sigma'}(\mathbf{k}_2) \mu_{\sigma''} E_{\sigma''}(\mathbf{k}_3) + \mu_{\sigma'} E_{\sigma'}(\mathbf{k}_3) \mu_{\sigma''} E_{\sigma''}(\mathbf{k}_2) \right) \kappa(t, T) \quad (4.15)$$

with

$$\kappa(t, T) = \Theta(t)\Theta(T)C(t, 0) + \Theta(t+T)\Theta(-T)C(t, T). \quad (4.16)$$

The helicity of the diffracted polarization depends on the individual contributions, as *mixed* in Eq. (4.13).

We discuss in more detail a type-I excitation. Corrections due to phase-space filling are neglected. The three-pulse experiment in Fig. 3 can clearly distinguish between correlations between opposite-spin excitons and parallel-spin excitons. In the cross-polarized configuration, pulses (2) and (3) have opposite helicity. The response in  $\mathbf{k}_f$ -direction has opposite helicity with respect to pulse (1). This is a consequence of angular-momentum conservation. In the case of equal helicity, all three pulses and the response have identical helicity. In both cases, the main difference comes from the type of heavy-hole correlation function, which enters the calculation of  $C(t, T)$ . Since the response comes from identical optical transitions, besides the helicity, we set  $\mu_\sigma E_\sigma \in \{0, 1\}$ . The responses in both polarization configurations differ mainly in the type of correlation function to be calculated. For the  $\pm$ -heavy-hole exciton transition, we find for  $\mathbf{k}_1 \rightarrow \bar{\sigma}$ ,  $\mathbf{k}_2 \rightarrow \sigma$  and  $\mathbf{k}_3 \rightarrow \bar{\sigma}$ , in the cross-polarized configuration and  $\mathbf{k}_i \rightarrow \sigma$  in the co-polarized configuration ( $\bar{\sigma} = -\sigma$ )

$$P_\sigma^{(3)}(t) = -ie^{-i(\omega_\sigma - i\Gamma)(t+T)} \kappa(t, T) \begin{cases} e^{i(\omega_{\bar{\sigma}} + \omega_\sigma)T} & \text{cross-circular,} \\ e^{i(\omega_\sigma + \omega_\sigma)T} & \text{co-circular.} \end{cases} \quad (4.17)$$

For resonant excitation, i.e.,  $\omega_\sigma = 0$ , the time-resolved phase of the polarization can be read off  $P^{(3)} = |P^{(3)}|e^{i\Phi}$  [55],

$$\begin{aligned}\Phi(t) = & -\Theta(t+T)\Theta(-T)tan^{-1}\left(\frac{ReC(t,T)}{ImC(t,T)}\right) \\ & - \Theta(t)\Theta(T)tan^{-1}\left(\frac{ReC(t,0)}{ImC(t,0)}\right),\end{aligned}\tag{4.18}$$

in the case where probe pulse (1) comes after the excitation with pulses (2) and (3),  $T < 0$ , and the case where pulse (1) precedes the excitation, i.e.,  $T > 0$ . For small times  $t$  after the excitation, the instantaneous phase-space-filling term leads to a  $\pi/2$ -phase shift of the polarization with respect to the external field  $E$ , as discussed in [18].

The observed quantities are the time-resolved (TR) intensity

$$\begin{aligned}I^{(3)}(t, T) &= |P_{\sigma}^{(3)}(t)|^2 \\ &= e^{-2\Gamma(T+t)}|\kappa(t, T)|^2\end{aligned}\tag{4.19}$$

and the time-integrated (TI) intensity

$$I^{(3)}(T) = \int_{-\infty}^{\infty} |P_{\sigma}^{(3)}(t, T)|^2 dt.\tag{4.20}$$

We have performed numerical simulations using a one-dimensional extended Hubbard model with long-range Coulomb interaction as defined in Appendix B. We present in this section the exact numerical calculations for this simple model and consider in the next section various approximations involving truncation of the summation in Eq. (4.13) for more complicated models. For resonant excitation, the ultrafast polarization dynamics is strongly affected by the relation between the exciton dephasing parameter  $\Gamma$  and the Rydberg energy  $\omega_x$ , since the detuning is zero. The Rydberg energy does not appear explicitly, but for the Coulomb interaction  $\tilde{U} \sim \omega_x$  holds. The results can be compared with few-level models on FWM [24].

The source term  $C(t, T)$  of Eq. (4.13) plays a central role in the nonlinear response, since it determines the nontrivial polarization dynamics. Many-particle correlation leads to a dynamical structure which is absent in a simplified non-interacting two-level system. Fig. 4 shows the typical source term for the parallel-spin case. The mean-field source term shows a finite rise time which corresponds to the finite rise time of the time-resolved nonlinear polarization signal, roughly the dephasing time  $T_2$ . For larger times, the nearly constant source term leads to an exponential decay of the resulting TR-signal in Eq. (4.15). The mean-field picture is considerably changed when the exact correlations are taken into account. Fig. 4 shows the following characteristic features: (1) an increase in the rise time of the signal compared to the mean-field approximation, (2) the signal exhibits a phase dynamics, and (3) the asymptotic value is complex and differs considerably from the mean-field value. Only in the extremely large dephasing limit, not shown in the figure, the correlation result approaches the mean-field value  $i\beta/2\Gamma$ .

Fig. 5 shows the typical source term for the case of opposite-spin correlation. The existence of a bound-state biexciton has a strong influence on the nonlinear response. Oscillations with the biexciton binding frequency of the single bound-state in the one-dimensional model are visible in Fig. 5. The energy denominator in Eq. (4.13) favors low-energy resonances, i.e., isolated bound-states ( $\omega_m < 0$ ) and the low-energy scattering-states continuum. It is important to note that the oscillations decay with twice the polarization decay-time  $T_2 = \Gamma^{-1}$  in the approximation of Sec. II. In the TR-signal, the oscillating contribution to

the signal should, therefore, be fairly small on the decaying part of the signal. The second, more important, observation is that, from Eq. (4.13) and the spectrum in Fig. 2, the biexciton resonance alone is responsible for the oscillations. This is a *ringing* phenomenon, which is *different* from the usual quantum-beat picture which is suggested by the few-level model [22,20].

Fig. 6 shows the results for the time-resolved polarization for zero delay  $T = 0$  and weak dephasing. The solid line shows the mean-field calculation, which obviously gives a poor approximation for resonant excitation and small dephasing. The exact result for cross-polarized circular excitation shows the ringing of the intensity signal with the biexciton binding frequency, which is already present in the source term in Fig. 5. The signal for co-polarized excitation is of the same order of magnitude but shows no oscillatory behavior. The signal peaks at roughly  $T_2/2$ , which is less than estimated previously [20].

In Fig. 7, a shorter dephasing time of  $T_2 = 0.5$  ps is assumed. The mean-field result looks better in comparison with the co-polarized signal. The exact signals have a decreased rise time of the maximum, which can be explained by an additional dephasing mechanism due to the superposition of the continuum of two-exciton states, which leads to a natural *intrinsic decay*, similar to the effect of an inhomogeneously broadened system.

The time-integrated signal in Fig. 8 shows the effect of finite delays between the *exciting* pulses (2) and (3) and the *probe* pulse (1). The result of the numerical simulation is in very good agreement with the experimental results by Wang et al. [20], who have performed a three-pulse FWM experiment on a *GaAs* quantum-well system. The figure shows the strong decrease of the co-polarized signal for negative time delay, which is due to the enhanced intrinsic dephasing of the continuum of two-exciton scattering states. The cross-polarized signal is stronger for negative time delay, which indicates the effect of quasi-bound excitonic molecules. The spectral weight of the correlation function in Fig. 2 (b) for parallel-spin excitons is more enhanced in the low-frequency regime. This leads to a stronger total signal in Eq. (4.15), which can be reproduced for different dephasing parameters.

Fig. 9 shows the time-integrated intensity of the FWM-signal for co-polarized circular excitation for different dephasing times. For short dephasing time, we recover the well-known mean-field behavior for homogeneously broadened systems, which predicts a rise of the signal  $\sim T_2/4$  and a decay of the signal  $\sim T_2/2$  [1,2]. This can be explained by simply counting the number of polarization-waves which are present before the nonlinear signal is emitted. For positive time-delay, even for a longer dephasing time, the decay  $\sim T_2$  can be observed because correlation effects influence only the strength of the time-integrated signal. For negative time-delay, significant deviation from the  $\sim T_2/4$ -law is found. The probe pulse interacts with the delay  $-T > 0$  and fast decaying modes of the correlations cannot be sustained. *The calculated results show a smooth transition from a steep rise near zero delay time, where correlations with the fast modes of the spectrum of two-exciton scattering states are important, to a regime where low-energy modes dominate the response.* The latter again shows the asymptotic mean-field like  $\sim T_2/4$  dependence.

The most prominent feature of the cross-polarized response in Fig. 10 is the *modulation* of the signal with the binding-frequency of the bound-state molecule at negative time delay. This biexcitonic-effect has been observed experimentally by various groups [16,22] and has sparked much theoretical effort to improve the mean-field theory of the semiconductor Bloch equations. This signature clearly shows the importance of correlations, which cannot be

neglected for the resonant excitation of the 1s-exciton in semiconductor heterostructures. No signal in the cross-polarized configuration is predicted by the mean-field approximation. For shorter dephasing times, the modulations disappear very quickly and the signal shows similar behavior compared to the co-polarized geometry. We also observe a decrease of the modulations, if the pulse-width is increased. The biexcitonic-modulations (if a bound-state molecule exists) can only be observed for sufficient short laser pulses and weak dephasing of the coherence (polarization) in semiconductors. However, none of the above conditions is necessary to observe correlations due to the two-exciton scattering-continuum, which is always present and gives the main contribution, if bound-states are absent because of impurity-scattering, interface effects, etc. The correlation function approach gives a unified description of the observable effects. In principle the same treatment can be applied to type-II and type-III excitations, but the large number of terms involved renders the computation quite tedious. Much work still has to be done. A discussion of further specific nonlinear optical experiments where correlations are involved is in progress.

## V. APPROXIMATIONS AND COMPARISON WITH RELATED APPROACHES

In considering possible applications of the correlation function approach for an improved treatment of the dynamical nonlinear response, we need a tractable response theory which takes into account, for example, (i) non-resonant, above band-gap excitations where electron-electron scattering becomes important and where the Markovian approximation is no longer valid on short time scales, (ii) coherent and non-coherent scatterings with LO-phonons, and (iii) applied magnetic field in heterostructures. Some theoretical work has already been done in deriving scattering-rate corrections with memory kernels for the SBE [56], in LO-phonon corrections [57,58], and in high magnetic fields [32]. In semiconductor heterostructures or bulk systems, the calculation of the force-force correlation function, even for resonant excitation, is an enormous numerical task because of the four-body problem involved. For systems beyond the simple models for which the exact calculations are possible as described in the last two sections, we develop various approximation schemes to incorporate correlation beyond the mean-field level in the dynamical optical response for low-density excitation.

### A. Excitation induced dephasing (EID)

EID corrections for the SBE have been discussed by Wang et al. [47] in an application to FWM, where a phenomenological, density dependent and  $\mathbf{k}$ -diagonal dephasing-parameter was introduced. We can derive a similar correction from the exact third-order contributions to the nonlinear response. In this case, the contribution originates entirely from exciton-exciton correlation.

Extracting the fast time-dependence of the linear polarization in Eq. (2.17)

$$X_{1,n,\sigma}^{(1)}(t) = e^{-i\omega_{1,n,\sigma}t} \tilde{X}_{1,n,\sigma}^{(1)}(t) \quad (5.1)$$

and the correlation function, c.f. Eq. (4.8), we find for the correlation part of Eq. (2.31)

$$\begin{aligned}
& \int_{-\infty}^t e^{-2\Gamma(t-t')} F_{\tilde{n},\tilde{\sigma};n,\sigma}^{n',\sigma';n'',\sigma''}(t-t') X_{1,n',\sigma'}^{(1)}(t') X_{1,n'',\sigma''}^{(1)}(t') dt' \\
&= e^{-i(\omega_{1,n',\sigma'} + \omega_{1,n'',\sigma''})t} \int_{-\infty}^t e^{-2\Gamma(t-t')} \tilde{F}_{\tilde{n},\tilde{\sigma};n,\sigma}^{n',\sigma';n'',\sigma''}(t-t') \tilde{X}_{1,n',\sigma'}^{(1)}(t') \tilde{X}_{1,n'',\sigma''}^{(1)}(t') dt' \\
&\rightarrow \tilde{\gamma}_{\tilde{n},\tilde{\sigma};n,\sigma}^{n',\sigma';n'',\sigma''} X_{1,n',\sigma'}^{(1)}(t) X_{1,n'',\sigma''}^{(1)}(t).
\end{aligned} \tag{5.2}$$

Hence, we have identified:

$$\tilde{\gamma}_{\tilde{n},\tilde{\sigma};n,\sigma}^{n',\sigma';n'',\sigma''} = \int_0^\infty e^{-2\Gamma\tau} \tilde{F}_{\tilde{n},\tilde{\sigma};n,\sigma}^{n',\sigma';n'',\sigma''}(\tau) d\tau, \tag{5.3}$$

a microscopic expression for the EID for the low-density optical regime. The imaginary part of  $\tilde{\gamma}$  renormalizes the mean-field parameter  $\beta$ . The real part of  $\tilde{\gamma}$  leads to a *dephasing* of the nonlinear polarization, which can be seen from Eq. (2.31). In addition to the phenomenological treatment [47], polarization-mixing is now also automatically taken into account.

### B. Short-time memory approximation

In the limit of large dephasing, a short-time approximation of the memory kernel in Eq. (5.2) is valid by Eq. (2.28),

$$F_{\tilde{n},\tilde{\sigma};n,\sigma}^{n',\sigma';n'',\sigma''}(\tau) \rightarrow \gamma_{\tilde{n},\tilde{\sigma};n,\sigma}^{n',\sigma';n'',\sigma''} + \mathcal{O}(\tau). \tag{5.4}$$

Thus, we obtain a correlation-modified complex mean-field parameter, which exhibits polarization mixing and leads to EID:

$$\tilde{\gamma}_{\tilde{n},\tilde{\sigma};n,\sigma}^{n',\sigma';n'',\sigma''} \rightarrow \frac{\gamma_{\tilde{n},\tilde{\sigma};n,\sigma}^{n',\sigma';n'',\sigma''}}{2\Gamma}. \tag{5.5}$$

We observe that, for diagonal contributions, e.g.,  $n = n' = a$  and  $\tilde{n} = n'' = b$ , the expression Eq. (5.5) is positive. Hence, the nonlinear polarization for, say  $a$ , has an effective dephasing which depends on the density of species  $b$  given by

$$\Gamma_a \rightarrow \Gamma_a + \frac{\gamma_{a,b}}{\Gamma_a + \Gamma_b} X_b^* X_b > 0. \tag{5.6}$$

Explicit results for the expectation value  $\gamma_{a,b}$  are given in Appendix A.

### C. Non-interacting excitons approximation

We propose an approximation scheme for the correlation function  $F$ , where we replace the time-evolution for the  $D$ -operator Eq. (B13) with the full Hamiltonian  $H$  of the biexciton subspace ( $N_p = 2$ ) with the free time-evolution of excitons. For more explicit results, we use the  $D$ -operator representation of Eq. (A13):

$$\begin{aligned}
F_{\tilde{n},\tilde{\sigma};n,\sigma}^{n',\sigma';n'',\sigma''}(\tau) \rightarrow & \sum_{\substack{\beta,\beta',\alpha,\alpha', \\ \mathbf{q} \neq 0, \mathbf{q}' \neq 0}} \tilde{U}_{\mathbf{q}} \tilde{U}_{-\mathbf{q}'} a_{n,\alpha}(\mathbf{q}) a_{\tilde{n},\alpha'}(-\mathbf{q}) a_{n',\beta}(-\mathbf{q}')^* a_{n'',\beta''}(\mathbf{q}')^* \\
& \times \langle 0 | B_{\alpha,\sigma}(\mathbf{q}) B_{\alpha',\tilde{\sigma}}(-\mathbf{q}) B_{\beta,\sigma'}^\dagger(-\mathbf{q}') B_{\beta',\sigma''}^\dagger(\mathbf{q}') | 0 \rangle \\
& \times e^{-i(\omega_{\beta,\sigma'}(\mathbf{q}') + \omega_{\beta',\sigma''}(\mathbf{q}'))\tau}.
\end{aligned} \tag{5.7}$$

This expression can be simplified further. We note that the expression Eq. (5.7) is a non-perturbative result which is exact to second order in the Coulomb interaction but properly includes all Coulomb effects to form excitons. If no bound-state biexcitons are present, this expression should give a reasonable approximation beyond the short-time memory approximation. The commutator in Eq. (5.7) is calculated in Eq. (A14). Since we are interested in the slowly varying contributions to  $F(\tau)$ , we restrict the remaining exciton summations in Eq. (5.7) to diagonal contributions, i.e.,  $\beta = n''$  and  $\beta' = n'$ . The summation cannot be performed analytically for finite  $\tau$ . According to Eq. (A14), we can split the correlation function into three contributions. The *bosonic* part gives

$$\begin{aligned}
F^{(1)} + F^{(2)} = & \sum_{\mathbf{q} \neq 0} \tilde{U}_{\mathbf{q}}^2 e^{-i(\omega_{n',\sigma'}(\mathbf{q}) + \omega_{n'',\sigma''}(\mathbf{q}))\tau} \\
& \times \left( f_{\tilde{n},n''}^{\tilde{\sigma}}(\mathbf{q}) f_{n,n'}^{\sigma}(-\mathbf{q}) f_{n'',n''}^{\sigma''}(\mathbf{q})^* f_{n',n'}^{\sigma'}(-\mathbf{q})^* \delta_{\sigma,\sigma'} \delta_{\tilde{\sigma},\sigma''} \right. \\
& \left. + f_{\tilde{n},n'}^{\tilde{\sigma}}(\mathbf{q}) f_{n,n''}^{\sigma}(-\mathbf{q}) f_{n'',n''}^{\sigma''}(-\mathbf{q})^* f_{n',n'}^{\sigma'}(\mathbf{q})^* \delta_{\tilde{\sigma},\sigma'} \delta_{\sigma,\sigma''} \right),
\end{aligned} \tag{5.8}$$

with the functions  $f$  defined in Eq.(A12). Due to the composite character of excitons, the third contribution is

$$\begin{aligned}
F^{(3)} = & - \sum_{\mathbf{q},\mathbf{k},\mathbf{k}'} \tilde{U}_{\mathbf{q}} \tilde{U}_{\mathbf{k}-\mathbf{k}'} e^{-i(\omega_{n',\sigma'}(\mathbf{q}) + \omega_{n'',\sigma''}(\mathbf{q}))\tau} \\
& \times \left( \delta_{\sigma,\sigma''}^{(c)} \delta_{\tilde{\sigma},\sigma'}^{(c)} \delta_{\sigma,\sigma'}^{(v)} \delta_{\tilde{\sigma},\sigma''}^{(v)} f_{n'',n''}^{\sigma''}(-\mathbf{q})^* f_{n',n'}^{\sigma'}(\mathbf{q})^* \right. \\
& + f_{n'',n''}^{\sigma''}(-\mathbf{q}) f_{n',n'}^{\sigma'}(\mathbf{q}) \delta_{\sigma,\sigma''}^{(v)} \delta_{\tilde{\sigma},\sigma'}^{(v)} \delta_{\sigma,\sigma'}^{(c)} \delta_{\tilde{\sigma},\sigma''}^{(c)} \Big) \\
& \times \left( \Phi_{\tilde{n},\mathbf{k}'+\mathbf{q},\tilde{\sigma}}^* - \Phi_{\tilde{n},\mathbf{k}+\mathbf{q},\tilde{\sigma}}^* \right) \left( \Phi_{n,\mathbf{k},\sigma}^* - \Phi_{n,\mathbf{k}',\sigma}^* \right) \Phi_{n'',\mathbf{k}'+\eta_{\sigma''}\kappa_{\sigma''}\mathbf{q},\sigma''} \Phi_{n',\mathbf{k}+\eta_{\sigma'}\mathbf{q},\sigma'}.
\end{aligned} \tag{5.9}$$

The Kronecker-delta is restricted to the conduction ( $c$ ) or valence-band ( $v$ ), respectively. Eq. (5.7) is a non-perturbative result and corresponds to the summation of a class of diagrams in the expansion of the correlation function. This can be useful in calculating the response from higher dimensional semiconductor models, which will be addressed in future work. The low-frequency range of the spectrum is approximated by Eq. (5.7), which corresponds to the long-time behavior of the correlation function and is dominant in the nonlinear optical response if no bound-state molecules are present. Higher-frequency modes naturally decay very fast, which affects the ultra short-time memory. Eqs. (5.8,5.9) can be calculated numerically with the exciton wave-functions as input.

#### D. Comparison with collision terms in the Boltzmann approximation

Finally, we want to approximate the correlation to second-order in the Coulomb interaction. This will enable us to make a qualitative comparison of the correlation-part of the

nonlinear optical response with semi-classical Boltzmann-Equation approaches. This is done here to third-order in the external field. We expand the *polarization* for a transition  $\sigma$  and Bloch vector  $\mathbf{k}$  in terms of excitons and inspect the source terms which gives the correlation corrections only. Since the force-force correlation function is already second-order in  $\tilde{U}_{\mathbf{q}}$ , we can use the non-interacting linear polarization Eq. (2.17)

$$\begin{aligned} X_{1,n,\sigma}^{(1)}(t) &= i\mu_{\sigma} \sum_{\mathbf{k}} \int_{-\infty}^t \langle E_{n,\sigma} | e^{-i(H-i\Gamma)(t-t')} | \mathbf{k}, \sigma \rangle E_{\sigma}(t') dt' \\ &\rightarrow i\mu_{\sigma} \sum_{\mathbf{k}} \Phi_{n,\mathbf{k},\sigma}^* \int_{-\infty}^t e^{-i(\epsilon_{\mathbf{k},\sigma}-i\Gamma)(t-t')} E_{\sigma}(t') dt' \\ &= \sum_{\mathbf{k}} \Phi_{n,\mathbf{k},\sigma}^* p_{\mathbf{k},\sigma}^{(1)}(t). \end{aligned} \quad (5.10)$$

The correlation source term in Eq. (2.31) to second order in the Coulomb interaction is

$$\begin{aligned} \dot{p}_{\mathbf{k},\sigma}^{(3)}(t) \Big|_{scatt} &:= \sum_n \Phi_{n,\mathbf{k},\sigma} \dot{P}_{n,\sigma}(t) \\ &= \frac{1}{2} \sum_{\substack{n,\tilde{n},\tilde{\sigma},n',\sigma',n'',\sigma'' \\ \mathbf{k}_1,\mathbf{k}_2,\mathbf{k}_3}} \Phi_{n,\mathbf{k},\sigma} \Phi_{\tilde{n},\mathbf{k}_1,\tilde{\sigma}} \Phi_{n',\mathbf{k}_2,\sigma'}^* \Phi_{n'',\mathbf{k}_3,\sigma''}^* \left( p_{\mathbf{k}_1,\tilde{\sigma}}^{(1)}(t) \right)^* \\ &\quad \times \int_{-\infty}^t e^{-2\Gamma(t-t')} F_{\tilde{n},\tilde{\sigma};n,\sigma}^{n',\sigma';n'',\sigma''}(t-t') p_{\mathbf{k}_2,\sigma'}^{(1)}(t') p_{\mathbf{k}_3,\sigma''}^{(1)}(t') dt'. \end{aligned} \quad (5.11)$$

The exciton summations can be performed to yield

$$\begin{aligned} &\sum_{\substack{n,\tilde{n},\tilde{\sigma},n',\sigma',n'',\sigma'' \\ \mathbf{k}_1,\mathbf{k}_2,\mathbf{k}_3}} \Phi_{n,\mathbf{k},\sigma} \Phi_{\tilde{n},\mathbf{k}_1,\tilde{\sigma}} \Phi_{n',\mathbf{k}_2,\sigma'}^* \Phi_{n'',\mathbf{k}_3,\sigma''}^* \\ &\times F_{\tilde{n},\tilde{\sigma};n,\sigma}^{n',\sigma';n'',\sigma''}(t-t') p_{\mathbf{k}_1,\tilde{\sigma}}^{(1)}(t)^* p_{\mathbf{k}_2,\sigma'}^{(1)}(t') p_{\mathbf{k}_3,\sigma''}^{(1)}(t') \\ &= \sum_{\mathbf{k}_1,\mathbf{k}_2,\mathbf{k}_3,\mathbf{q},\mathbf{q}'} \tilde{U}_{\mathbf{q}} \tilde{U}_{\mathbf{q}'} \\ &\times \langle 0 | c_{\mathbf{k}_1,\tilde{\sigma}_1}^{\dagger} c_{\mathbf{k}_1+\mathbf{q},\tilde{\sigma}_2} c_{\mathbf{k},\sigma_1}^{\dagger} c_{\mathbf{k}+\mathbf{q},\sigma_2} e^{-iH_0(t-t')} c_{\mathbf{k}_3+\mathbf{q}',\sigma_2'}^{\dagger} c_{\mathbf{k}_3,\sigma_1'}^{\dagger} c_{\mathbf{k}_2+\mathbf{q}',\sigma_2'} c_{\mathbf{k}_2,\sigma_1'} | 0 \rangle \\ &\times \left( p_{\mathbf{k}_1,\tilde{\sigma}}^{(1)}(t)^* p_{\mathbf{k}_2,\sigma'}^{(1)}(t') p_{\mathbf{k}_3,\sigma''}^{(1)} - p_{\mathbf{k}_1-\mathbf{q},\tilde{\sigma}}^{(1)}(t)^* p_{\mathbf{k}_2,\sigma'}^{(1)}(t') p_{\mathbf{k}_3,\sigma''}^{(1)} \right. \\ &\quad - p_{\mathbf{k}_1,\tilde{\sigma}}^{(1)}(t)^* p_{\mathbf{k}_2-\mathbf{q}',\sigma'}^{(1)}(t') p_{\mathbf{k}_3,\sigma''}^{(1)} - p_{\mathbf{k}_1,\tilde{\sigma}}^{(1)}(t)^* p_{\mathbf{k}_2,\sigma'}^{(1)}(t') p_{\mathbf{k}_3-\mathbf{q}',\sigma''}^{(1)} \\ &\quad + p_{\mathbf{k}_1,\tilde{\sigma}}^{(1)}(t)^* p_{\mathbf{k}_2-\mathbf{q}',\sigma'}^{(1)}(t') p_{\mathbf{k}_3-\mathbf{q}',\sigma''}^{(1)} + p_{\mathbf{k}_1-\mathbf{q},\tilde{\sigma}}^{(1)}(t)^* p_{\mathbf{k}_2,\sigma'}^{(1)}(t') p_{\mathbf{k}_3-\mathbf{q}',\sigma''}^{(1)} \\ &\quad \left. + p_{\mathbf{k}_1-\mathbf{q},\tilde{\sigma}}^{(1)}(t)^* p_{\mathbf{k}_2-\mathbf{q}',\sigma'}^{(1)}(t') p_{\mathbf{k}_3,\sigma''}^{(1)} - p_{\mathbf{k}_1-\mathbf{q},\tilde{\sigma}}^{(1)}(t)^* p_{\mathbf{k}_2-\mathbf{q}',\sigma'}^{(1)}(t') p_{\mathbf{k}_3-\mathbf{q}',\sigma''}^{(1)} \right) \\ &\quad - (\mathbf{k} \rightarrow \mathbf{k} - \mathbf{q}), \end{aligned} \quad (5.12)$$

with the non-interacting Hamiltonian  $H_0$  being used for the time evolution. The matrix element in Eq. (5.12) is divided into 4 contributions with a total of 64 terms, which can be simplified by symmetry arguments. Note that the *bosonic* contributions to the matrix element yield a  $\delta_{\mathbf{q},\pm\mathbf{q}'}$  factor. This reproduces the third-order limit of the collision terms which were previously derived [56]. This also corresponds to the *two-loop* diagrams in the diagrammatic approach [27]. However, the true *fermionic* contributions also appear,

which are relevant for the parallel-spin and coupled-spin case and correspond to the *one-loop* diagrams. These terms might not be present in the usual semi-classical treatment of the scattering rates. The correlation function approach naturally incorporates these effects on the four-particle level and gives the exact low-density results.

## VI. CONCLUSION

In this paper, we have presented a *unified* theory of exciton-exciton interaction effects in the third-order nonlinear optical response, using a correlation function approach [30]. The *electronic* problem (dynamics of the four interacting particles) is separated from the nonlinear *optical* problem. Furthermore, the correlation effects beyond the mean-field terms is explicitly represented by a two-exciton force-force correlation function. By means of this formalism, we are able to investigate the role of exciton-exciton correlations in the third-order polarization in an application to resonantly excited heavy-hole excitons in a semiconductor quantum well. The correlation functions are calculated numerically for a one-dimensional semiconductor model with long-range Coulomb interaction, without perturbative approximation. Their spectra exhibit isolated resonances due to bound-state biexcitons and continuum of two-exciton scattering states. Additional, more pronounced features appear for decreasing mass-ratio of electron to hole.

A three-pulse FWM configuration can distinguish between parallel-spin and opposite-spin correlations. For co-polarized excitations, we find a significant deviation from the expected mean-field  $\sim T_2/4$  rise of the time-integrated FWM-signal for negative time delays between the pulses in the weak dephasing regime. This can be explained by an ultrafast intrinsic decay of correlations due to two-exciton scattering states, since bound-state molecules are *absent* in the case of parallel-spin correlations. For strong dephasing, we recover the well known mean-field results [2]. The signal in the cross-polarized configuration is dominated by a modulation with the binding frequency of the bound-state biexciton in the system, which has been observed in various experiments [16,22]. These oscillations appear as a ringing of the biexciton mode in the time-resolved signal, as distinct from true quantum-beats. For positive time delays, the third-order response is close to the mean-field  $T_2/2$ -decay behavior. Polarization-mixing for cross-polarized excitations is purely a correlation effect [27], absent in the conventional mean-field approach using the semiconductor Bloch equations [6,11].

We have also derived generalized effective equations of motion for the polarization for laser excitation near the fundamental exciton resonance or the exciton continuum states. This is intended for a future application of the theory to more realistic semiconductor quantum-wells. The exact third-order equations are compared with the results of Boltzmann-type scattering corrections to the quantum-kinetic equations. The effective parameters entering the dynamics can be calculated in second order of the exciton-exciton interaction, provided only that the exciton states are known, which is possible for a large number of semiconductor systems.

The correlation function approach can be generalized to include additional interactions, such as spin-flipping scattering processes or the coupling to LO-phonons [58]. A further application of the correlation theory to spin-beating phenomena in diluted magnetic semiconductors for the pump-and-probe configuration [59] has been made [60].

## ACKNOWLEDGMENTS

One of the authors (Th. Ö.) acknowledges financial support by the Deutsche Forschungsgemeinschaft (DFG). This work was supported in part by the Sonderforschungsbereich SFB 345, Göttingen, and in part by the NSF Grant No. DMS 94-21966. We also wish to thank M. Z. Maialle, R. G. Ulbrich, G. Böhne and D. S. Chemla for useful discussions and comments.

## APPENDIX A: COMMUTATOR ALGEBRA FOR THE FORCE OPERATOR

In this Appendix we derive the operators and parameters defined in section II in terms of a semiconductor Hamiltonian,  $H \equiv H_0 + U$ , with an independent-electron part:

$$H_0 = \sum_{\mathbf{k}, s} \epsilon_{\mathbf{k}, s} c_{\mathbf{k}, s}^\dagger c_{\mathbf{k}, s} , \quad (\text{A1})$$

where  $c_{\mathbf{k}, s}^\dagger$  creates a Bloch electron with combined band and spin index  $s$  at wave-vector  $\mathbf{k}$ , and an electron-electron interaction term:

$$U = \frac{1}{2} \sum_{\mathbf{k}, s, \mathbf{k}', s', \mathbf{q} \neq 0} \tilde{U}_{\mathbf{q}, s, s'} c_{\mathbf{k}+\mathbf{q}, s}^\dagger c_{\mathbf{k}', s'}^\dagger c_{\mathbf{k}', s'} c_{\mathbf{k}, s} , \quad (\text{A2})$$

where  $\tilde{U}_{\mathbf{q}, s, s'}$  is the Coulomb matrix element.

The exciton operator  $B_{n, \sigma}$  of a given transition  $\sigma$  is associated with the relative motion wave function  $\phi_{n, \mathbf{k}, \sigma}$  at zero center-of-mass momentum:

$$B_{n, \sigma} = \sum_{\mathbf{k}} \phi_{n, \mathbf{k}, \sigma}^* c_{\mathbf{k}, s'}^\dagger c_{\mathbf{k}, s} . \quad (\text{A3})$$

The transition  $\sigma = \sigma(s, s')$  connects an electron from a valence band with combined band and spin label  $s'$  to a conduction band state with label  $s$ . The corresponding *pair*-operator  $c_{\mathbf{k}, s'}^\dagger c_{\mathbf{k}, s}$  is denoted in Sec. II as  $\psi_{\mathbf{k}, \sigma}$ . Optical selection rules determine whether the  $\sigma$ -transition is an optically allowed dipole transition with matrix element  $\mu_\sigma$  or a so-called *dark* transition. Dark states are connected to optically active states via a spin-flip process, which is assumed to be very slow on the time scales of interest. The selection rules also determine the corresponding helicity of the dipole transition.

The first step leading to the force operator  $D$  is the commutator  $C_{n, \sigma} = [B_{n, \sigma}, H]$ ,

$$\begin{aligned} C_{n, \sigma} = & \sum_{\mathbf{k}} (\epsilon_{\mathbf{k}, s_2} - \epsilon_{\mathbf{k}, s_1}) \phi_{n, \mathbf{k}, \sigma}^* c_{\mathbf{k}, s_2}^\dagger c_{\mathbf{k}, s_1} \\ & - \sum_{\mathbf{k}, \mathbf{q} \neq 0} \tilde{U}_{\mathbf{q}, s_1, s_2} \phi_{n, \mathbf{k}, \sigma}^* c_{\mathbf{k}+\mathbf{q}, s_2}^\dagger c_{\mathbf{k}+\mathbf{q}, s_1} + \sum_{\mathbf{k}, \mathbf{q} \neq 0} \tilde{U}_{\mathbf{q}, s_1, s_1} \phi_{n, \mathbf{k}, \sigma}^* c_{\mathbf{k}, s_2}^\dagger c_{\mathbf{k}, s_1} \\ & + \sum_{\mathbf{k}, \mathbf{k}', s, \mathbf{q} \neq 0} \left( \tilde{U}_{\mathbf{q}, s, s_2} \phi_{n, \mathbf{k}'-\mathbf{q}, \sigma}^* - \tilde{U}_{\mathbf{q}, s, s_1} \phi_{n, \mathbf{k}', \sigma}^* \right) c_{\mathbf{k}+\mathbf{q}, s}^\dagger c_{\mathbf{k}, s} c_{\mathbf{k}'-\mathbf{q}, s_1}^\dagger c_{\mathbf{k}', s_2} . \end{aligned} \quad (\text{A4})$$

Using  $c_{\mathbf{k}, s_1}^\dagger c_{\mathbf{k}, s_2} = \sum_{\tilde{n}} \phi_{\tilde{n}, \mathbf{k}, \sigma}^* B_{\tilde{n}, \sigma}$ , the Wannier equation for the exciton wave function simplifies the first three terms on the rhs of Eq. (A4):

$$\begin{aligned} \sum_{\mathbf{k}, \mathbf{k}'} & \left[ \left( \epsilon_{\mathbf{k}, s_2} - \epsilon_{\mathbf{k}, s_1} + \sum_{\mathbf{q} \neq 0} \tilde{U}_{\mathbf{q}, s_1, s_1} \right) \delta_{\mathbf{k}, \mathbf{k}'} - \tilde{U}_{\mathbf{k}-\mathbf{k}', s_1, s_2} (1 - \delta_{\mathbf{k}, \mathbf{k}'}) \right] \Phi_{\mathbf{k}, n, \sigma}^* \Phi_{\mathbf{k}', \tilde{n}, \sigma} \\ & = \omega_{1, n, \sigma} \delta_{n, \tilde{n}}, \end{aligned} \quad (\text{A5})$$

and, therefore,

$$\begin{aligned} C_{n, \sigma} & = \omega_{1, n, \sigma} B_{n, \sigma} \\ & + \sum_{\mathbf{k}, \mathbf{k}', s, \mathbf{q} \neq 0} \left( \tilde{U}_{\mathbf{q}, s, s_2} \phi_{n, \mathbf{k}'-\mathbf{q}, \sigma}^* - \tilde{U}_{\mathbf{q}, s, s_1} \phi_{n, \mathbf{k}', \sigma}^* \right) c_{\mathbf{k}+\mathbf{q}, s}^\dagger c_{\mathbf{k}, s} c_{\mathbf{k}'-\mathbf{q}, s_1}^\dagger c_{\mathbf{k}', s_2}. \end{aligned} \quad (\text{A6})$$

The force operator is given by the commutator  $D_{p, l; n, \sigma} = [B_{p, l}, C_{n, \sigma}]$ . The first contribution on the rhs of Eq. (A6) vanishes because  $[B_{p, l}, B_{n, \sigma}] = 0$ . Thus,

$$\begin{aligned} D_{p, l; n, \sigma} & = \sum_{\mathbf{k}, \mathbf{k}', \mathbf{q} \neq 0} \left( \tilde{U}_{\mathbf{q}, l_2, s_2} \phi_{n, \mathbf{k}'-\mathbf{q}, \sigma}^* - \tilde{U}_{\mathbf{q}, l_2, s_1} \phi_{n, \mathbf{k}', \sigma}^* \right) \phi_{p, \mathbf{k}+\mathbf{q}, l}^* \\ & - \left( \tilde{U}_{\mathbf{q}, l_1, s_2} \phi_{n, \mathbf{k}'-\mathbf{q}, \sigma}^* - \tilde{U}_{\mathbf{q}, l_1, s_1} \phi_{n, \mathbf{k}', \sigma}^* \right) \phi_{p, \mathbf{k}, l}^* \\ & \times c_{\mathbf{k}+\mathbf{q}, l_1}^\dagger c_{\mathbf{k}, l_2} c_{\mathbf{k}'-\mathbf{q}, s_1}^\dagger c_{\mathbf{k}', s_2}. \end{aligned} \quad (\text{A7})$$

The spin-independent Coulomb interaction leads to a further simplification. In terms of the operator

$$A_{n, \sigma}(\mathbf{q}) = \sum_{\mathbf{k}} \left( \phi_{n, \mathbf{k}-\mathbf{q}/2, \sigma}^* - \phi_{n, \mathbf{k}+\mathbf{q}/2, \sigma}^* \right) c_{\mathbf{k}-\mathbf{q}/2, s_1}^\dagger c_{\mathbf{k}+\mathbf{q}/2, s_2}, \quad (\text{A8})$$

the  $D$ -operator can be written in a compact form:

$$D_{p, l; n, \sigma} = \sum_{\mathbf{q} \neq 0} \tilde{U}_{\mathbf{q}} A_{p, l}(\mathbf{q}) A_{n, \sigma}(-\mathbf{q}). \quad (\text{A9})$$

The  $A$ -operator can be related to excitons with finite center-of-mass momentum  $\mathbf{Q}$ . The mass ratio of electrons and holes play a crucial in the correlation function dynamics. We define for the transition  $\sigma = (s, s')$  the positive mass-ratio  $\kappa_\sigma = m_s/m_{s'}$ . With

$$\eta_\sigma = \frac{1}{1 + \kappa_\sigma} \quad (\text{A10})$$

the generalization of Eq. (A3) reads

$$B_{n, \sigma}(\mathbf{Q}) = \sum_{\mathbf{k}} \phi_{n, \mathbf{k}, \sigma}^* c_{\mathbf{k}-\eta_\sigma \mathbf{Q}, s'}^\dagger c_{\mathbf{k}+\kappa_\sigma \eta_\sigma \mathbf{Q}, s}. \quad (\text{A11})$$

We have neglected a possible  $\mathbf{Q}$ -dependence of the relative-motion wave-function, which is valid for parabolic bands. Transforming the eh representation in Eq. (A8) to one in terms of the excitons leads to

$$\begin{aligned} A_{n, \sigma}(\mathbf{q}) & = \sum_{\mathbf{k}, \alpha} \left( \phi_{n, \mathbf{k}-\eta_\sigma \mathbf{q}, \sigma}^* - \phi_{n, \mathbf{k}+\eta_\sigma \kappa_\sigma \mathbf{q}, \sigma}^* \right) \phi_{\alpha, \mathbf{k}, \sigma} B_{\alpha, \sigma}(\mathbf{q}) \\ & = \sum_{\alpha} f_{n, \alpha}^\sigma(\mathbf{q}) B_{\alpha, \sigma}(\mathbf{q}). \end{aligned} \quad (\text{A12})$$

The  $D$ -operator in Eq. (A9) becomes in terms of the excitons:

$$D_{p,l;n,\sigma} = \sum_{\alpha,\alpha',\mathbf{q} \neq 0} \tilde{U}_{\mathbf{q}} f_{p,\alpha}^l(\mathbf{q}) f_{n,\alpha'}^\sigma(-\mathbf{q}) B_{\alpha,l}(\mathbf{q}) B_{\alpha',\sigma}(-\mathbf{q}). \quad (\text{A13})$$

We use  $\tilde{U}_{\mathbf{q}} = \tilde{U}_{-\mathbf{q}}$ , to ensure the symmetry of the  $D$ -operator in the exciton labels.

The initial value  $\tau = 0$  of the correlation function Eq. (4.13) is a ground-state (vacuum) expectation value. We first calculate

$$\begin{aligned} & \langle 0 | B_{\alpha',\tilde{\sigma}}(\mathbf{q}) B_{\alpha,\sigma}(-\mathbf{q}) B_{\beta,\sigma''}^\dagger(-\mathbf{q}') B_{\beta',\sigma'}^\dagger(\mathbf{q}') | 0 \rangle \\ &= \delta_{\alpha',\tilde{\sigma};\beta,\sigma''} \delta_{\alpha,\sigma;\beta',\sigma'} \delta_{\mathbf{q},-\mathbf{q}'} + \delta_{\alpha',\tilde{\sigma};\beta',\sigma'} \delta_{\alpha,\sigma;\beta,\sigma''} \delta_{\mathbf{q},\mathbf{q}'} \\ &+ \langle 0 | B_{\alpha',\tilde{\sigma}}(\mathbf{q}) [B_{\alpha,\sigma}(-\mathbf{q}), B_{\beta,\sigma''}^\dagger(-\mathbf{q}')] B_{\beta',\sigma'}^\dagger(\mathbf{q}') | 0 \rangle. \end{aligned} \quad (\text{A14})$$

The initial value  $\gamma_{\tilde{n},\tilde{\sigma};n,\sigma}^{n',\sigma';n'',\sigma''}$  of Eq. (4.13) can be split in three contributions. The first term on the rhs of Eq. (A14) gives

$$\gamma^{(1)} = \delta_{\sigma,\sigma'} \delta_{\tilde{\sigma},\sigma''} \sum_{\beta,\beta',\mathbf{q}} \tilde{U}_{\mathbf{q}}^2 f_{\tilde{n},\beta}^{\tilde{\sigma}}(\mathbf{q}) f_{n,\beta'}^\sigma(-\mathbf{q}) f_{n'',\beta}^{\sigma''}(\mathbf{q})^* f_{n',\beta'}^{\sigma'}(-\mathbf{q})^*. \quad (\text{A15})$$

The summation over the exciton labels  $\beta, \beta'$  can be performed, using the abbreviation

$$\begin{aligned} g_{n,m}^\sigma(\mathbf{q}) &= \sum_{\beta} f_{n,\beta}^\sigma(\mathbf{q}) f_{m,\beta}^\sigma(\mathbf{q})^* \\ &= \sum_{\mathbf{k}} \left( \phi_{n,\mathbf{k}-\eta_\sigma \mathbf{q},\sigma}^* - \phi_{n,\mathbf{k}+\eta_\sigma \kappa_\sigma \mathbf{q},\sigma}^* \right) \left( \phi_{m,\mathbf{k}-\eta_\sigma \mathbf{q},\sigma} - \phi_{m,\mathbf{k}+\eta_\sigma \kappa_\sigma \mathbf{q},\sigma} \right), \end{aligned} \quad (\text{A16})$$

which gives

$$\gamma^{(1)} = \delta_{\sigma,\sigma'} \delta_{\tilde{\sigma},\sigma''} \sum_{\mathbf{q}} \tilde{U}_{\mathbf{q}}^2 g_{\tilde{n},n''}^{\tilde{\sigma}}(\mathbf{q}) g_{n,n'}^\sigma(-\mathbf{q}) \quad (\text{A17})$$

and for the second term on the rhs of Eq. (A14)

$$\gamma^{(2)} = \delta_{\sigma,\sigma''} \delta_{\tilde{\sigma},\sigma'} \sum_{\mathbf{q}} \tilde{U}_{\mathbf{q}}^2 g_{\tilde{n},n'}^{\tilde{\sigma}}(\mathbf{q}) g_{n,n''}^\sigma(-\mathbf{q}). \quad (\text{A18})$$

The third contribution arises only if the two electron-hole pairs have at least one band in common, i.e., in the parallel-spin or coupled-spin case, c.f. Sec. III. In the case of excitons being ideal *bosons*, only  $\gamma^{(1)}$  and  $\gamma^{(2)}$  would contribute. We give the result for the general case:

$$\begin{aligned} \gamma^{(3)} &= - \left( \delta_{\sigma,\sigma''}^{(c)} \delta_{\tilde{\sigma},\sigma'}^{(c)} \delta_{\sigma,\sigma'}^{(v)} \delta_{\tilde{\sigma},\sigma''}^{(v)} + \delta_{\sigma,\sigma''}^{(v)} \delta_{\tilde{\sigma},\sigma'}^{(v)} \delta_{\sigma,\sigma'}^{(c)} \delta_{\tilde{\sigma},\sigma''}^{(c)} \right) \sum_{\mathbf{q},\mathbf{k},\mathbf{k}'} \tilde{U}_{\mathbf{q}} \tilde{U}_{\mathbf{k}-\mathbf{k}'} \\ &\times (\Phi_{\tilde{n},\mathbf{k}'-\mathbf{q}/2,\tilde{\sigma}}^* - \Phi_{\tilde{n},\mathbf{k}'+\mathbf{q}/2,\tilde{\sigma}}^*) (\Phi_{n'',\mathbf{k}'-\mathbf{q}/2,\sigma''} - \Phi_{n'',\mathbf{k}-\mathbf{q}/2,\sigma''}) \\ &\times (\Phi_{n',\mathbf{k}+\mathbf{q}/2,\sigma'} - \Phi_{n',\mathbf{k}'+\mathbf{q}/2,\sigma'}) (\Phi_{n,\mathbf{k}+\mathbf{q}/2,\sigma}^* - \Phi_{n,\mathbf{k}-\mathbf{q}/2,\sigma}^*). \end{aligned} \quad (\text{A19})$$

The Kronecker-delta symbol with an upper index means, the corresponding conduction ( $c$ ) or valence-band ( $v$ ) must be identical for the transition pair.

## APPENDIX B: AN INTERACTING SEMICONDUCTOR MODEL

We present the details of the real-space extended Hubbard-model used for the numerical calculations of the correlation-function and the linear optical properties (excitons). We start with the general  $d$ -dimensional lattice-model of an electron-hole system and briefly review the fundamental aspects of the problem on a lattice. The kinetic energy part of a two-band lattice model is the usual hopping term

$$H_0 = \sum_{\mathbf{m}, \mathbf{m}', s} t_{\mathbf{m}, \mathbf{m}'}^{(s)} c_{\mathbf{m}, s}^\dagger c_{\mathbf{m}', s} + h.c., \quad (\text{B1})$$

where  $c_{\mathbf{m}', s}^\dagger$  creates an electron in a Wannier-state at the lattice site  $\mathbf{m}$  with a combined band and spin index  $s$  and  $t_{\mathbf{m}, \mathbf{m}'}^{(s)}$  is the hopping matrix element between two sites. The hopping is restricted to nearest neighbor with parameter  $t^{(s)}$  for each band. We take  $t^{(s)} < 0$  ( $t^{(s)} > 0$ ) for an s-type (p-type) conduction (valence) band, allowing for interband optical transitions. The potential energy of the system is given by the Coulomb interaction between the electrons and charge-positive lattice ions with charge  $eZ_{core} > 0$ . In terms of the dimensionless charge-density (electrons and ions) at site  $\mathbf{m}$

$$\rho_{\mathbf{m}} = \left( \sum_s c_{\mathbf{m}, s}^\dagger c_{\mathbf{m}, s} \right) - Z_{core}, \quad (\text{B2})$$

the Coulomb interaction in the Wannier-states to leading order is given by the electrostatic monopole-monopole contribution

$$\hat{U} = \frac{1}{2} \sum_{\mathbf{m}, \mathbf{m}'} U_{\mathbf{m}, \mathbf{m}'} \rho_{\mathbf{m}} \rho_{\mathbf{m}'}. \quad (\text{B3})$$

where  $U_{\mathbf{m}, \mathbf{m}'} = e^2/|\mathbf{m} - \mathbf{m}'|$  for different sites and the on-site Coulomb interaction  $U_{\mathbf{m}, \mathbf{m}} \equiv U_0$  is an additional parameter in the model.

The ground-state  $|0\rangle$  of the lattice model is given by the completely filled valence-band states at each site. For the numerical calculation of the correlation function, a four-band approximation of the semiconductor is sufficient, i.e., only two holes and two electrons of one or two species are relevant. The index  $s$  is split into two bands and two spin directions. This leads to different types of correlation functions, as discussed in Sec. III. We write the ground state as

$$|0\rangle = \prod_{\mathbf{m}} c_{\mathbf{m}, 1, \uparrow}^\dagger c_{\mathbf{m}, 1, \downarrow}^\dagger |vac\rangle. \quad (\text{B4})$$

The spatial extension of the relative motion of a *single* exciton in its ground state depends on the ratio of the sum of the bandwidths  $B_s \equiv B_1 + B_2 = 2d(t_1 - t_2)$  and the nearest neighbor Coulomb energy  $U_1 \equiv e^2/a_L$ , where  $a_L$  is the lattice constant. For  $B_s/U_1 \gg 1$  the results of the lattice model are similar to the continuum limit given by the usual two-parabolic-band effective-mass model. If one expands the band dispersion quadratically around the center of the Brillouin zone one finds for the Bohr radius of the exciton for  $d = 3$

$$a_0 = \frac{2(t_1 - t_2)}{U_1} a_L \quad (\text{B5})$$

and the exciton binding energy  $\omega_x$  is given by

$$\omega_x = \frac{U_1}{2} \left( \frac{a_L}{a_0} \right). \quad (\text{B6})$$

In the following, we give all energies in units of the Rydberg energy  $\omega_x$ . One should keep in mind that this is *not* the exciton binding energy in  $d = 1$ , which apart from a different dimensionless prefactor depends on the ratio  $\eta \equiv U_0/U_1$ . The different effective electron (hole) masses enter via  $|t_1/t_2| = |m_2/m_1|$ . The total Hamiltonian operator  $H = H_0 + \hat{U}$  is conveniently transformed into the electron-hole picture defining  $c_{\mathbf{m},s} = c_{\mathbf{m},2,s}$  for electron states and  $h_{\mathbf{m},s} = c_{\mathbf{m},1,s}^\dagger$  for the hole states. Let  $|\Phi\rangle$  denote a many-particle eigenstate of  $H$  with an arbitrary number  $N_p$  of the eh-pairs as a quantum-number. As the corresponding pair-number operator  $N_p$  commutes with  $H$ , we can always work with eigenstates of  $N_p$ . This is the fundamental assumption for the Hubbard-operator formulation of the Hamiltonian in Sec. II.

We now discuss in detail the results of the numerical calculations for a quasi-one-dimensional ring model. The Coulomb interaction Eq. (B3) between two charges depends on the chord-distance [61]

$$|\mathbf{m} - \mathbf{m}'| = \frac{Na_L}{\pi} \sin\left[\frac{\pi}{N}|m - m'|\right] \quad (\text{B7})$$

of the sites, which are labeled by the dimensionless numbers  $m$ . The model interpolates smoothly between the two limits of Frenkel excitons  $a_0/a_L \rightarrow 0$  and the Wannier limit of large extended objects  $a_0/a_L \gg 1$ , which is only limited by the finite total system size  $N$ . The system size for the numerical calculation of the correlation function is  $N = 120$  for equal-spin correlation and  $N = 140$  for opposite-spin correlation. The on-site Coulomb interaction is fixed with  $\eta = 1.5$ . We have also fixed the bandwidth  $B := |4(t_2 - t_1)|$  of the eh-pair continuum for each model, which depends only on the reduced electron and hole mass, while the positive mass ratio  $m_e/m_h$  is varied. The mass ratio is an important parameter of the two eh-pair subspace. We compare the positronium limit  $m_e/m_h = 1$  with the semiconductor *GaAs* case of  $m_e/m_h \approx 0.15$  and the molecular (hydrogen) limit  $m_e/m_h \ll 1$ . The long-range Coulomb potential leads to the formation of a finite number of bound exciton-states in the system in contrast to the usual Hubbard-model with purely on-site repulsion  $U_0$ .

### 1. Parallel-spin excitons

The parallel-spin exciton case is characterized by the exchange repulsion between same type carriers in the bands, which, in an ideal one-dimensional system, plays the role of dynamical boundary conditions. The parallel-spin case is relevant when the optical excitation process is limited to a single circularly polarization of the external field. A complete set of parallel-spin two-pair states with zero center of mass momentum is given by [61]

$$|p, \alpha, \beta\rangle = \frac{C_p^{(\alpha,\beta)}}{\sqrt{N}} \sum_m c_{m+p+\alpha}^\dagger h_{m+p}^\dagger c_{m+\beta}^\dagger h_m^\dagger |0\rangle, \quad (\text{B8})$$

where

$$C_p^{(\alpha,\beta)} = \begin{cases} \sqrt{2} & p = N/2 \text{ and } \alpha = \beta \\ 1 & \text{else} \end{cases} \quad (\text{B9})$$

is a normalization constant and a triplet  $(p, \alpha, \beta)$  labels the relative position of the carriers. In order to avoid double counting of states, the set of possible triplets is restricted. The (single) spin-index is understood.

The real-space representation of the product state of two excitons with quantum numbers  $a$  and  $b$  with band indices  $(a_2, a_1)$  and  $(b_2, b_1)$ , which enters the calculation of the generating correlation function, is given by

$$M_{a,b}^\dagger |0\rangle = \frac{1}{N} \sum_{m_1, m_2, m_3, m_4} \phi_b(m_1 - m_2) \phi_a(m_3 - m_4) \times c_{m_1, b_1}^\dagger h_{m_2, b_2}^\dagger c_{m_3, a_1}^\dagger h_{m_4, a_2}^\dagger |0\rangle, \quad (\text{B10})$$

where each exciton has zero center-of-mass momentum. The real-space exciton wavefunction is given by

$$\phi_{a,k} = \frac{1}{\sqrt{N}} \sum_m e^{-ikm} \phi_a(m), \quad (\text{B11})$$

and the exciton operator can be expressed as

$$B_a^\dagger = \frac{1}{\sqrt{N}} \sum_{m_1, m_2} \phi_a(m_1 - m_2) c_{m_1, a_1}^\dagger h_{m_2, a_2}^\dagger. \quad (\text{B12})$$

For the force-force correlation function in the nonlinear optical response, we need a linear superposition of two-pair states in the initial state  $D_{a,b}^\dagger |0\rangle$

$$D_{a,b}^\dagger |0\rangle = \frac{1}{N} \sum_{m_1, m_2, m_3, m_4} \phi_b(m_1 - m_2) \phi_a(m_3 - m_4) \times (U_{m_3 - m_1} - U_{m_4 - m_1} - U_{m_3 - m_2} + U_{m_4 - m_2}) \times c_{m_1, b_1}^\dagger h_{m_2, b_2}^\dagger c_{m_3, a_1}^\dagger h_{m_4, a_2}^\dagger |0\rangle. \quad (\text{B13})$$

Both states are center-of-mass eigenstates with zero total momentum in systems with periodic boundary conditions. It is possible to fix the hole position  $m_4$  and to introduce relative distances with respect to this hole to reduce the number of coordinates. The states Eq. (B10) and Eq. (B13) can then be expressed in the basis set Eq. (B8).

## 2. Opposite-spin excitons

The corresponding basis set for the opposite-spin pair-states is chosen as

$$|m_1, m_2, m_3\rangle = \frac{1}{\sqrt{N}} \sum_{m_4} c_{m_3 + m_4, a_1}^\dagger h_{m_2 + m_4, a_2}^\dagger c_{m_1 + m_4, b_1}^\dagger h_{m_4, b_2}^\dagger |0\rangle, \quad (\text{B14})$$

where the opposite-spin indices for the carriers in one band are understood, i.e.,  $b_2 \neq a_2$  and  $b_1 \neq a_1$ . For numerical work, the absence of the Pauli-blocking for the two electrons/holes in the bands leads to a quite simple counting of opposite-spin states in contrast to the equal-spin case.

The numerical evaluation proceeds in the usual way. The total number of basis states involved in the calculation is  $N^3$  for the opposite-spin problem, which gives a vector length of about  $3 \times 10^6$ . The Lanczos algorithm requires two states for the iteration, which reside in memory to speed up the process and can be handled quite well on a PC with a total of 64 MByte memory. The Lanczos algorithm tridiagonalizes the Hamiltonian for the 4-particle problem, starting with the (normalized) initial state  $D^\dagger|0\rangle$  for the force-force correlation function. Each iteration step produces one new basis state. The iteration is extremely fast, due to the sparseness of the Hamiltonian matrix of  $H$  in real-space. We truncate the iteration after the spectrum of the resolvent matrix  $(z - H)^{-1}$  stabilizes. No eigenvectors or eigenvalues for the biexciton problem have to be calculated. The relevant spectrum is given in the usual way

$$f_{a,b}(\omega) = -2Im\langle 0|D_{a,b}\frac{1}{\omega - H + i0}D_{a,b}^\dagger|0\rangle \quad (\text{B15})$$

from the inversion of the resolvent matrix, which is simple in the tridiagonal representation of  $H$ .

## REFERENCES

- [1] K. Leo, M. Wegener, J. Shah, D. S. Chemla, E. O. Göbel, T. C. Damen, S. Schmitt-Rink, and W. Schäfer, Phys. Rev. Lett. **65**, 1340 (1990).
- [2] M. Wegener, D. S. Chemla, S. Schmitt-Rink, and W. Schäfer, Phys. Rev. A **42**, 5675 (1990).
- [3] S. Schmitt-Rink, D. Bennhardt, V. Heuckeroth, P. Thomas, P. Haring, G. Maidorn, H. Bakker, K. Leo, D.-S. Kim, J. Shah, and K. Köhler, Phys. Rev. B **46**, 10460 (1992).
- [4] S. Weiss, M.-A. Mycek, J.-Y. Bigot, S. Schmitt-Rink, and D. S. Chemla, Phys. Rev. Lett. **69**, 2685 (1992).
- [5] D.-S. Kim, J. Shah, T. C. Damen, W. Schäfer, F. Jahnke, S. Schmitt-Rink, and K. Köhler, Phys. Rev. Lett. **69**, 2725 (1992).
- [6] H. Haug and S. W. Koch, *Quantum Theory of the Optical and Electronic Properties of Semiconductors*, (World Scientific, Singapore, 1993) 2nd ed.
- [7] D. G. Steel, H. Wang, M. Jiang, K. Ferrio, and S. Cundiff, in *Coherent Optical Interactions in Semiconductors*, edited by R. T. Phillips (Plenum, New York, 1994), p. 157.
- [8] D. S. Chemla, Solid State Comm. **92**, 37 (1994).
- [9] E. O. Göbel, *Festkörperprobleme* (Advances in Solid State Physics), edited by U. Rössler (Vieweg, Braunschweig, 1990) Vol. 30, p. 269.
- [10] S. Schmitt-Rink and D. Chemla, Phys. Rev. Lett. **57**, 2752 (1986).
- [11] M. Lindberg and S.W. Koch, Phys. Rev. B **38**, 3342 (1988).
- [12] W. Schäfer, *Festkörperprobleme* (Advances in Solid State Physics), edited by U. Rössler (Vieweg, Braunschweig, 1988) Vol. 28, p. 63.
- [13] R. Zimmermann and M. Hartmann, Phys. Stat. Sol. (b) **38**, 3342 (1988).
- [14] I. Balslev, R. Zimmermann, and A. Stahl, Phys. Rev. B **40**, 4095 (1989).
- [15] R. Binder, S.W. Koch, M. Lindberg, N. Peyghambarian, and W. Schäfer, Phys. Rev. Lett. **65**, 899 (1990); R. Binder, S. W. Koch, M. Lindberg, W. Schäfer, and F. Jahnke, Phys. Rev. B **43**, 6520 (1991).
- [16] G. Finkelstein, S. Bar-Ad, O. Carmel, I. Bar-Joseph, and Y. Levison, Phys. Rev. B **47**, 12964 (1993).
- [17] D. Bennhardt, P. Thomas, R. Eccleston, E. J. Mayer, and J. Kuhl, Phys. Rev. B **47**, 13485 (1993).
- [18] J.-Y. Bigot, M.-A. Mycek, S. Weiss, R. G. Ulbrich, and D. S. Chemla, Phys. Rev. Lett. **70**, 3307 (1993); D. S. Chemla, J.-Y. Bigot, M.-A. Mycek, S. Weiss, and W. Schäfer, Phys. Rev. B, **50**, 8439 (1994).
- [19] S. T. Cundiff, M. Koch, W. H. Knox, J. Shah, and W. Stolz, Phys. Rev. Lett. **77**, 1107 (1996).
- [20] H. Wang, J. Shah, T. C. Damen, and L. N. Pfeiffer, Solid State Comm. **91**, 869 (1994).
- [21] D. J. Lovering, R. T. Phillips, G. J. Denton, and G. W. Smith, Phys. Rev. Lett. **68**, 1880 (1992).
- [22] E. J. Mayer, G. O. Smith, V. Heuckeroth, J. Kuhl, K. Bott, A. Schulze, T. Meier, D. Bennhardt, S. W. Koch, P. Thomas, R. Hey, and K. Ploog, Phys. Rev. B **50**, 14730 (1994).
- [23] G. Bartels, V. M. Axt, K. Victor, A. Stahl, P. Leisching, and K. Köhler, Phys. Rev. B **51**, 11217 (1995).

- [24] K. Bott, O. Heller, D. Bennhardt, S. T. Cundiff P. Thomas, E. J. Mayer, G. O. Smith, R. Eccleston, J. Kuhl, and K. Ploog, Phys. Rev. B **48**, 17418 (1993).
- [25] V. M. Axt and A. Stahl, Zeitschrift für Physik B **93**, 195 (1994); 205 (1994).
- [26] E. J. Mayer, G. O. Smith, V. Heuckeroth, J. Kuhl, K. Bott, A. Schulze, T. Meier, S. W. Koch, P. Thomas, R. Hey, and K. Ploog, Phys. Rev. B **51**, 10909 (1995).
- [27] M. Z. Maialle and L. J. Sham, Phys. Rev. Lett. **73**, 3310 (1994).
- [28] M. Lindberg, Y. Z. Hu, R. Binder, and S. W. Koch, Phys. Rev. B **50**, 18060 (1994).
- [29] V. M. Axt, A. Stahl, E. J. Mayer, P. Haring Bolivar, S. Nüsse, K. Ploog, and K. Köhler, Phys. Stat. Sol. B **188**, 447 (1995).
- [30] Th. Östreich, K. Schönhammer, and L. J. Sham, Phys. Rev. Lett. **74**, 4698 (1995).
- [31] W. Schäfer et al., Phys. Rev. **53**, 16429 (1996).
- [32] P. Kner et al., Phys. Rev. Lett. **78**, 1319 (1997).
- [33] M. Combescot and R. Combescot, Phys. Rev. Lett. **61**, 117 (1988); Phys. Rev. B **40**, 3788 (1989).
- [34] M. Combescot, Phys. Rev. B **41**, 3517 (1990).
- [35] L. Allen and J. H. Eberly, *Optical Resonance and Two-Level Atoms*, (Wiley and Sons, New York, 1975).
- [36] G. S. Agarwal, *Quantum Optics*, edited by G. Höhler, Springer Tracts in Modern Physics Vol.70 (Springer, New York, 1974).
- [37] C. Cohen-Tannoudji, J. Dupont-Roc, and G. Grynberg, *Atom-Photon Interactions*, (Wiley, New York, 1992).
- [38] S. Mukamel, in *Molecular Nonlinear Optics*, edited by J. Zyss (Academic Press, New York, 1994).
- [39] S. Schmitt-Rink, D. S. Chemla, and H. Haug, Phys. Rev. B **37**, 941 (1988).
- [40] H. Haug and S. Schmitt-Rink, Prog. Quant. Electr. **9**, 3 (1984).
- [41] W. Hanke and L. J. Sham, Phys. Rev. B **21**, 4656 (1980).
- [42] J. R. Kuklinski and S. Mukamel, Phys. Rev. B **42**, 2959 (1990).
- [43] Th. Östreich and A. Knorr, Phys. Rev. B **50**, 5717 (1994).
- [44] M. Lindberg, R. Binder, and S.W. Koch, Phys. Rev. A **45**, 1865 (1992).
- [45] Th. Östreich and A. Knorr, Phys. Rev. B **48**, 17811 (1993); A. Knorr, Th. Östreich, K. Schönhammer, R. Binder, and S. W. Koch, Phys. Rev. B **49**, 14024 (1994).
- [46] L. J. Sham, M. Z. Maialle, Th. Östreich, and K. Schönhammer, Nuovo Cimento **17 D**, 1315 (1995).
- [47] H. Wang, K. B. Ferrio, D. G. Steel, P. R. Berman, Y. Z. Hu, R. Binder, and S. W. Koch, Phys. Rev. A **49**, R1551 (1994).
- [48] D. B. Tran Thoai and H. Haug, Zeitschrift für Physik B **91**, 199 (1993).
- [49] G. Mahan, *Many-particle physics*, (Plenum, New York, 1981).
- [50] L. V. Keldysh and A. N. Kozlov, Zh. Eksp. Teor. Fiz. **54**, 978 (1968) [Sov. Phys. -JETP **27**, 521 (1968)].
- [51] E. Hanamura, J. Phys. Soc. Jpn. **37**, 1545 (1974), **37**, 1553 (1974).
- [52] R. Zimmermann, in *Many-Particle Theory of Highly Excited Semiconductors*, Teubner Texte zur Physik Vol. 18, (Teubner, Leipzig, 1987) and references therein.
- [53] J. K. Cullum, R. A. Willoughby, *Lanczos Algorithms for Large Symmetric Eigenvalue Computations* Vol. 1, (Birkhäuser, Boston, 1985).
- [54] T. Yajima and Y. Taira, J. Phys. Soc. Jpn. **47**, 1620 (1979).

- [55] Th. Östreich, K. Schönhammer, and L. J. Sham, *Proc. Intern. Conf. Phys. Semicond.* **23**, 765 (World Scientific, Singapore, 1996).
- [56] L. Bányai, D. B. Tran Thoai, E. Reitsamer, H. Haug, D. Steinbach, M. U. Wehner, M. Wegener, T. Marschner, and W. Stolz, *Phys. Rev. Lett.*, **75**, 2188 (1995).
- [57] A. V. Kuznetsov, *Phys. Rev. B* **44**, 13381 (1991).
- [58] V. M. Axt, K. Victor, and A. Stahl, *Phys. Rev. B* **53**, 7244 (1996).
- [59] J. J. Baumberg, D. D. Awschalom, N. Samarth, H. Luo, and J. K. Furdyna, *Phys. Rev. Lett.* **72**, 717 (1994).
- [60] Th. Östreich, K. Schönhammer, and L. J. Sham, *Phys. Rev. Lett.* **75**, 2554, (1995).
- [61] Th. Östreich and K. Schönhammer, *Solid State Comm.* **85**, 629 (1993).

## FIGURES

FIG. 1. Selection rules of heavy and light-hole exciton transitions in Zincblende structures. A splitting of heavy- and light-hole states in heterostructures allows for a selected excitation of these transitions (I). The degenerate case (II) is shown for each helicity of the exciting field. The  $\Lambda$ -transition (III) is excited by linear polarization.

FIG. 2. Force-force correlation function spectra  $F(\omega)$  for the  $1s$ -exciton contribution for opposite spins (solid line) and parallel spins (dashed line). The mass-ratio of electrons and holes is  $m_e/m_h = 1$  for (a), which corresponds to the *positronium* limit,  $m_e/m_h = 0.15$  for (b), which corresponds to the heavy-hole/electron mass ratio of *GaAs* and for the *molecular* (hydrogen) limit  $m_e/m_h = 0$  in (c). Bound excitonic molecules appear for  $\omega < 0$  and continuum two-exciton contribution have  $\omega > 0$ .

FIG. 3. Three-pulse four-wave-mixing transmission geometry.

FIG. 4. Source term  $C(t, 0)$  in the nonlinear response in the parallel-spin case with parameters of Fig. 5). The mean-field approximation, which has no real part from Eq. (4.14) overestimates the response.

FIG. 5. Source term  $C(t, 0)$  for the nonlinear response in the opposite-spin case with the spectral function of Fig. 2 (b). The dephasing time is  $T_2 = 2$  ps. The pronounced oscillations with a period of 2.8 ps ( $E_{xx} = 1.5$  meV) origin from the bound-state biexciton in the system.

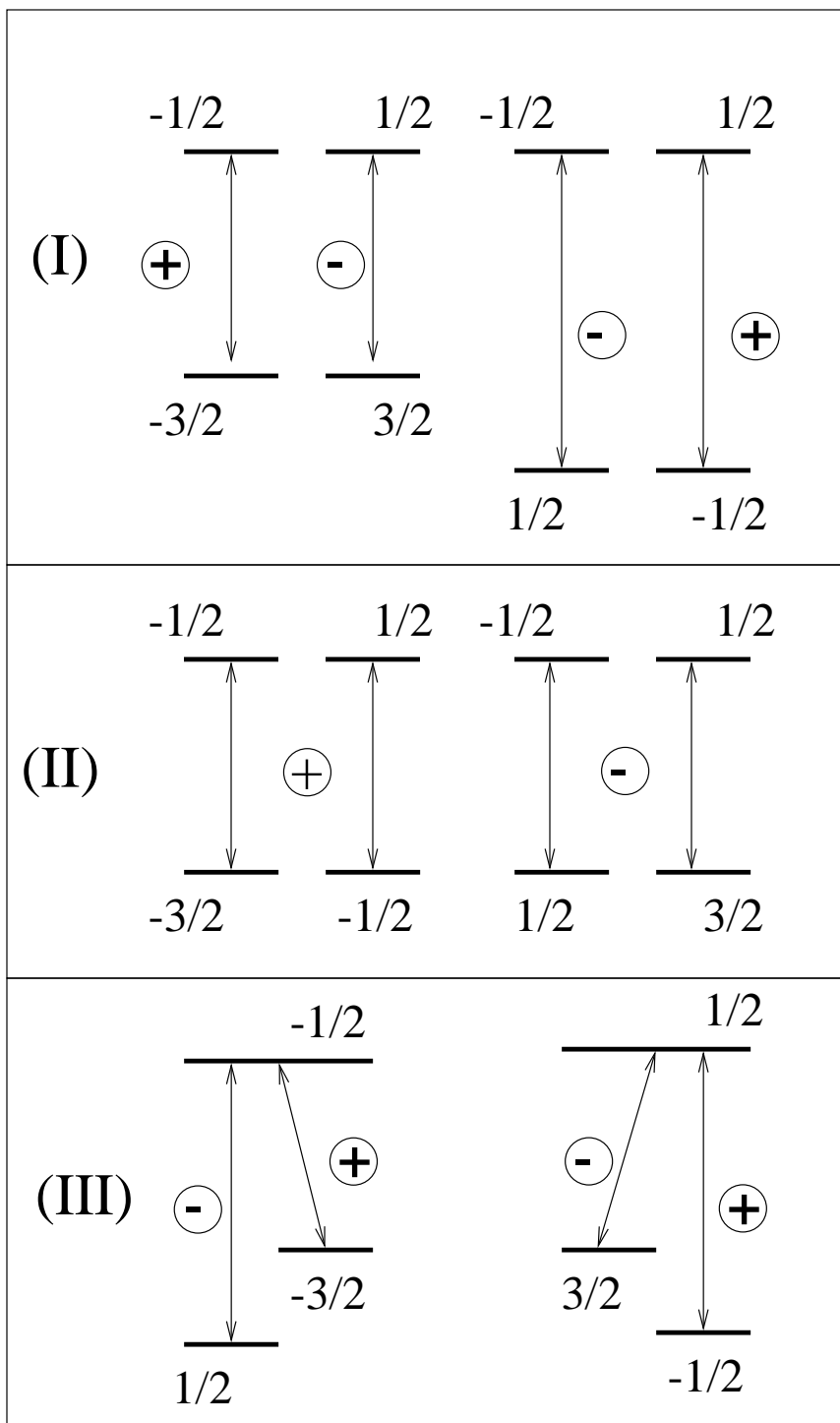
FIG. 6. TR-signal of the nonlinear polarization for the one-dimensional semiconductor model for  $T = 0$  in the weak dephasing limit. The oscillations with the biexciton binding energy are a ringing in the signal, since no additional biexciton states are necessary for the response. The dephasing time is  $T_2 = 4$  ps.

FIG. 7. TR-signal of the nonlinear polarization for the one-dimensional semiconductor model for  $T = 0$  in the strong dephasing limit in comparison with the mean-field response for parallel-spin excitation. The dephasing time is  $T_2 = 0.5$  ps.

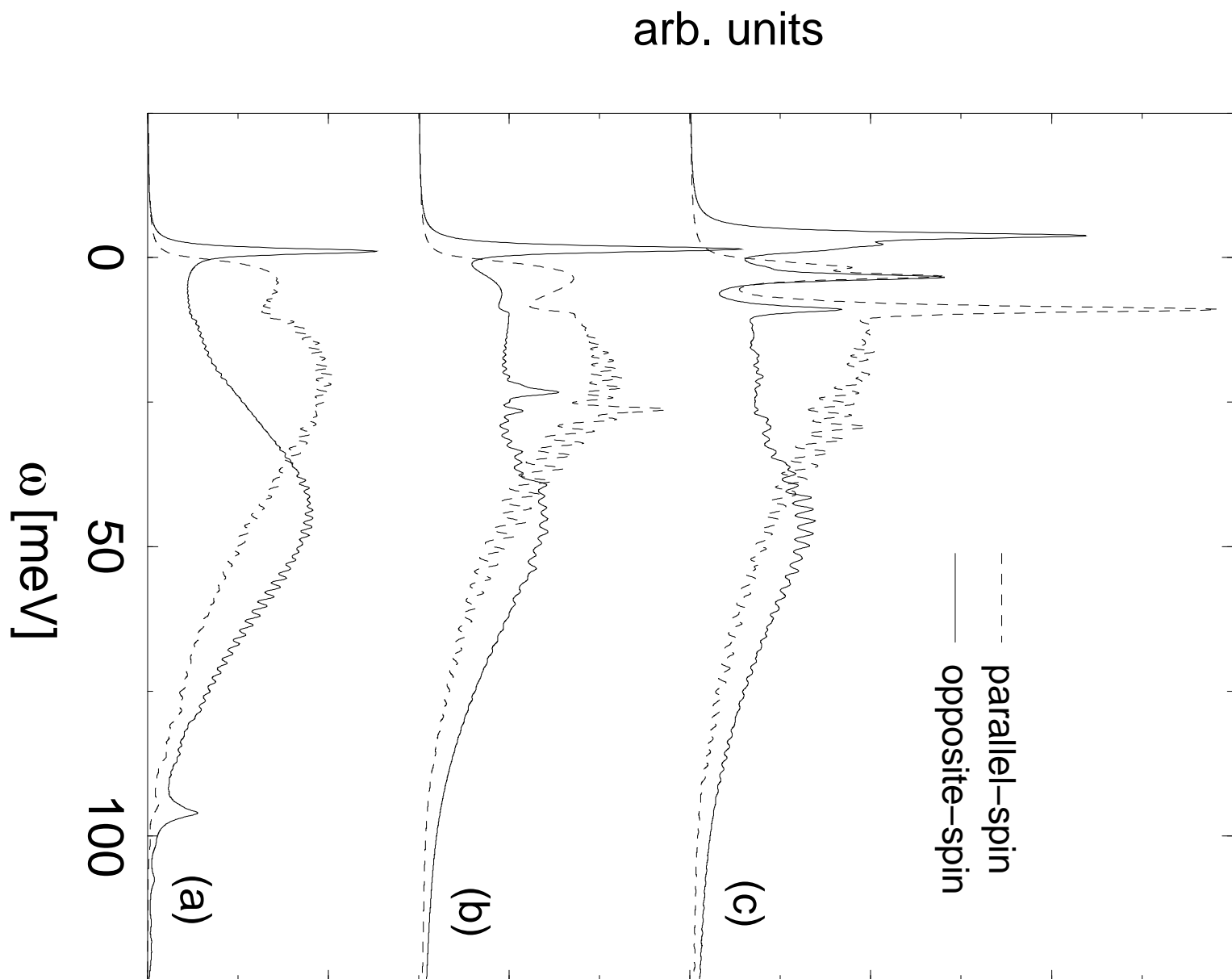
FIG. 8. TI-intensity of the FWM-signal for co-polarized (solid line) and cross-polarized (dashed line) circular excitation for a dephasing time of  $T_2 = 4$  ps.

FIG. 9. Normalized TI-intensity of the FWM-signal for co-polarized circular excitation on a log scale. For negative time delay, significant deviation from the exponential decay with a rise-time of  $T_2/4$  is observed for smaller dephasing.

FIG. 10. Normalized TI-intensity of the FWM-signal for cross-polarized circular excitation on a log scale. For negative delay times, oscillations with the binding energy of the biexciton are visible for sufficiently small dephasing.



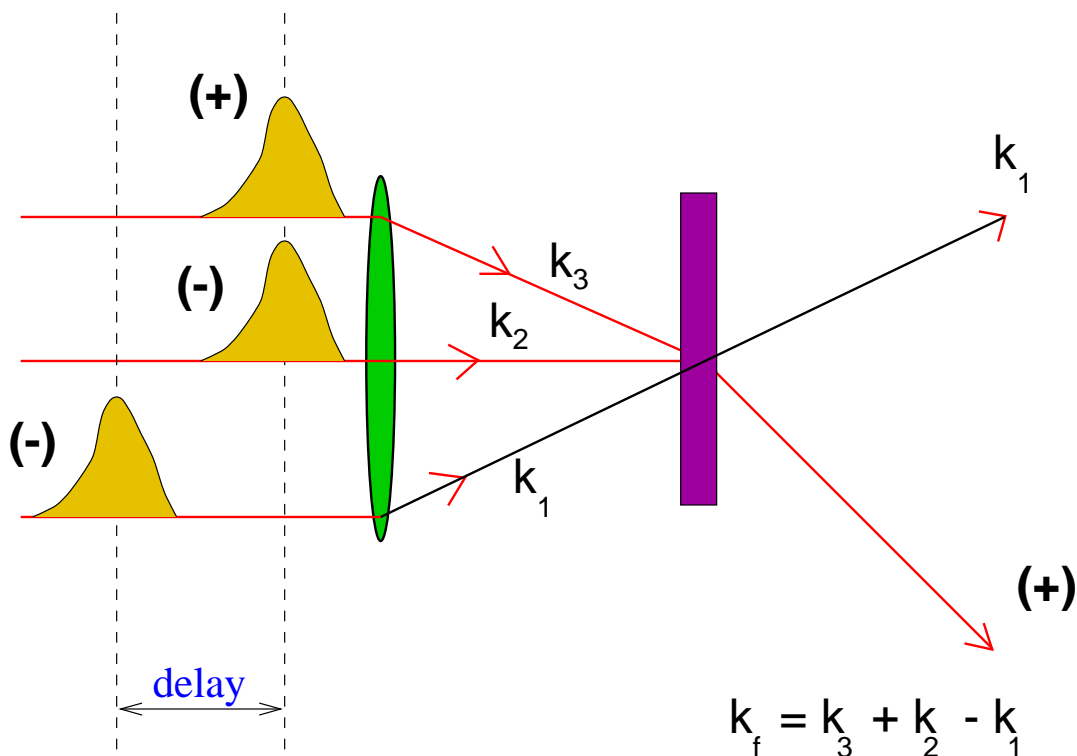
oestreich et al. theory of exciton-exciton correlation ... Figure 1

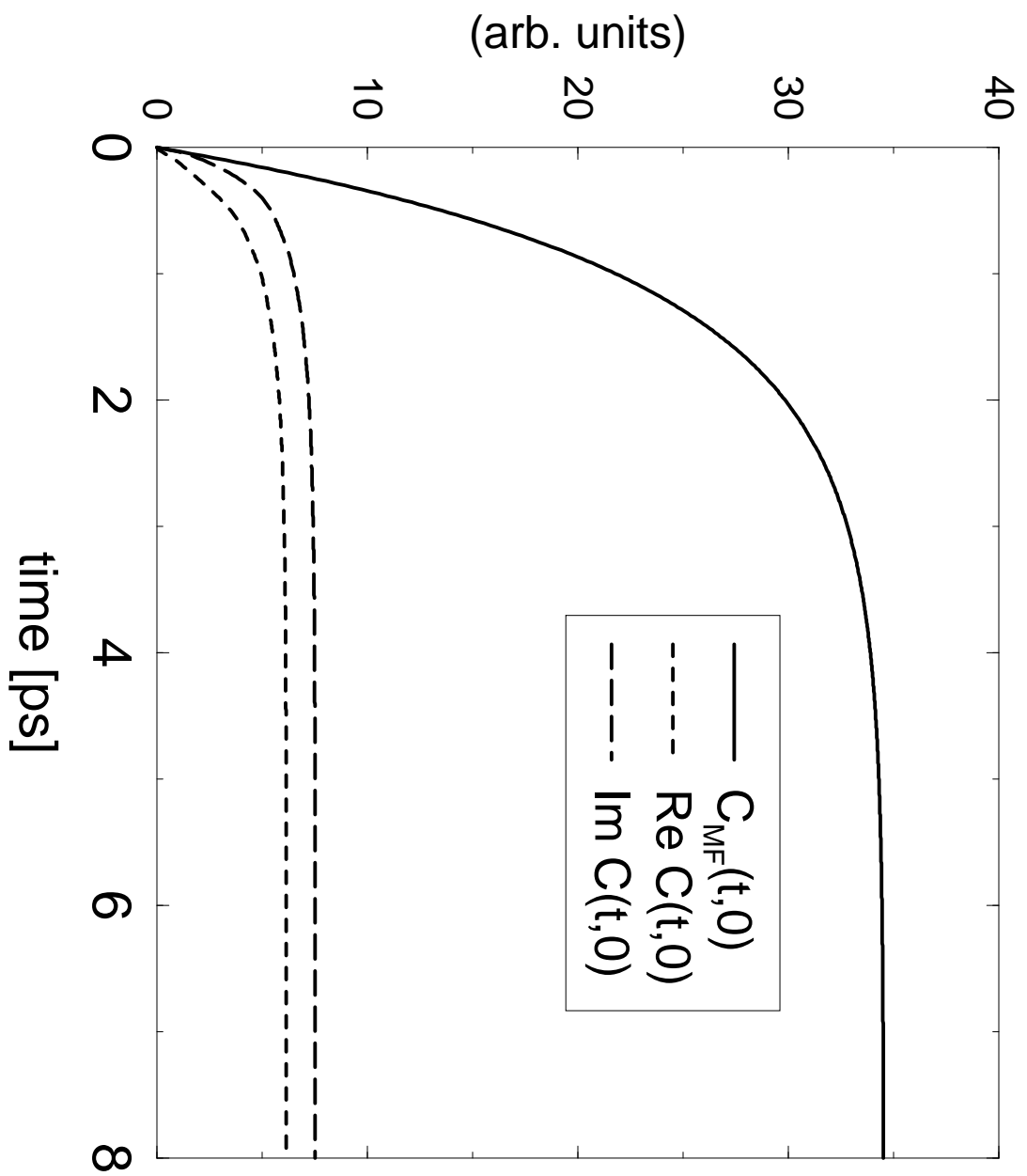


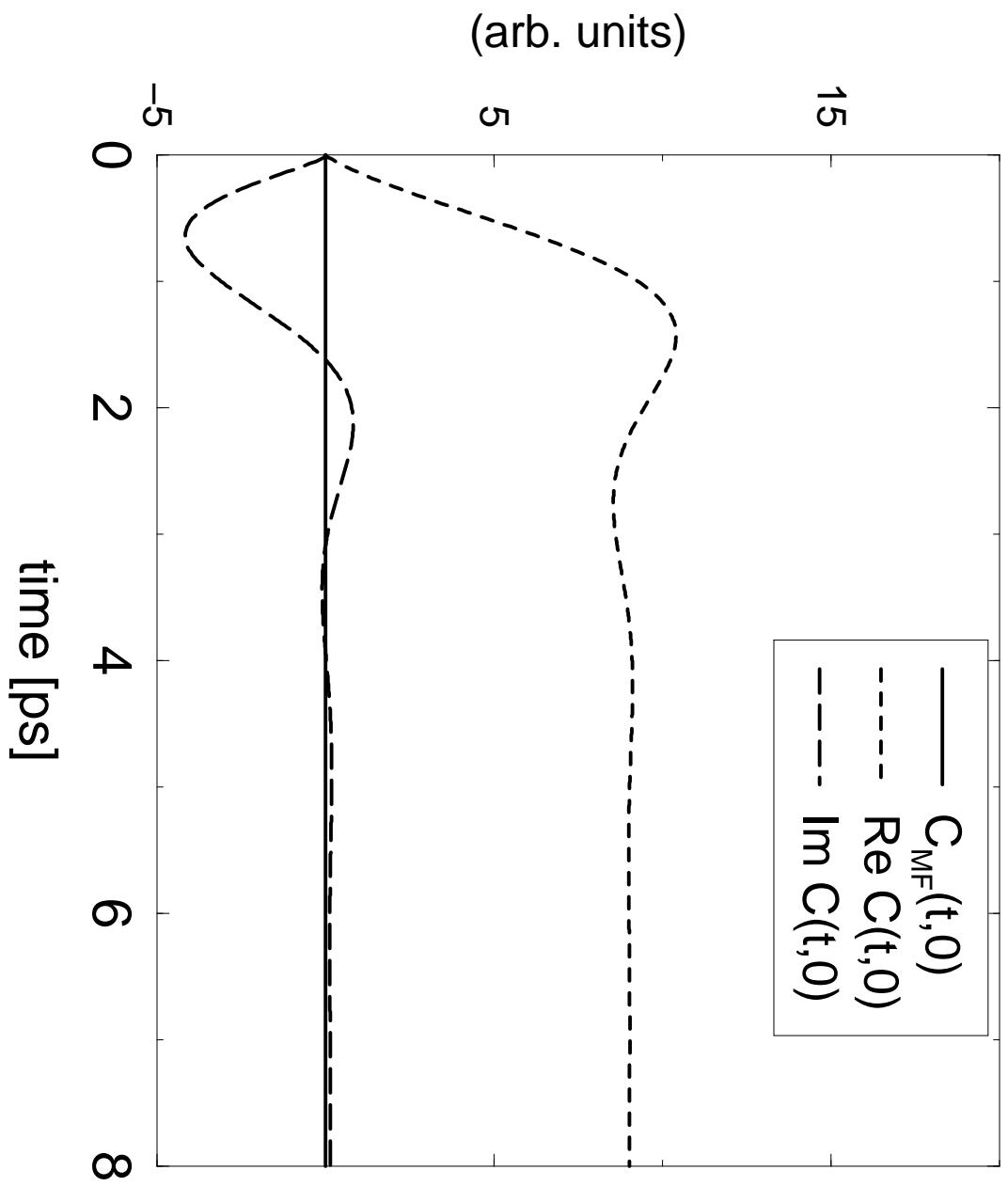
oestreich et al. : Theory of exciton – exciton ... Figure 2

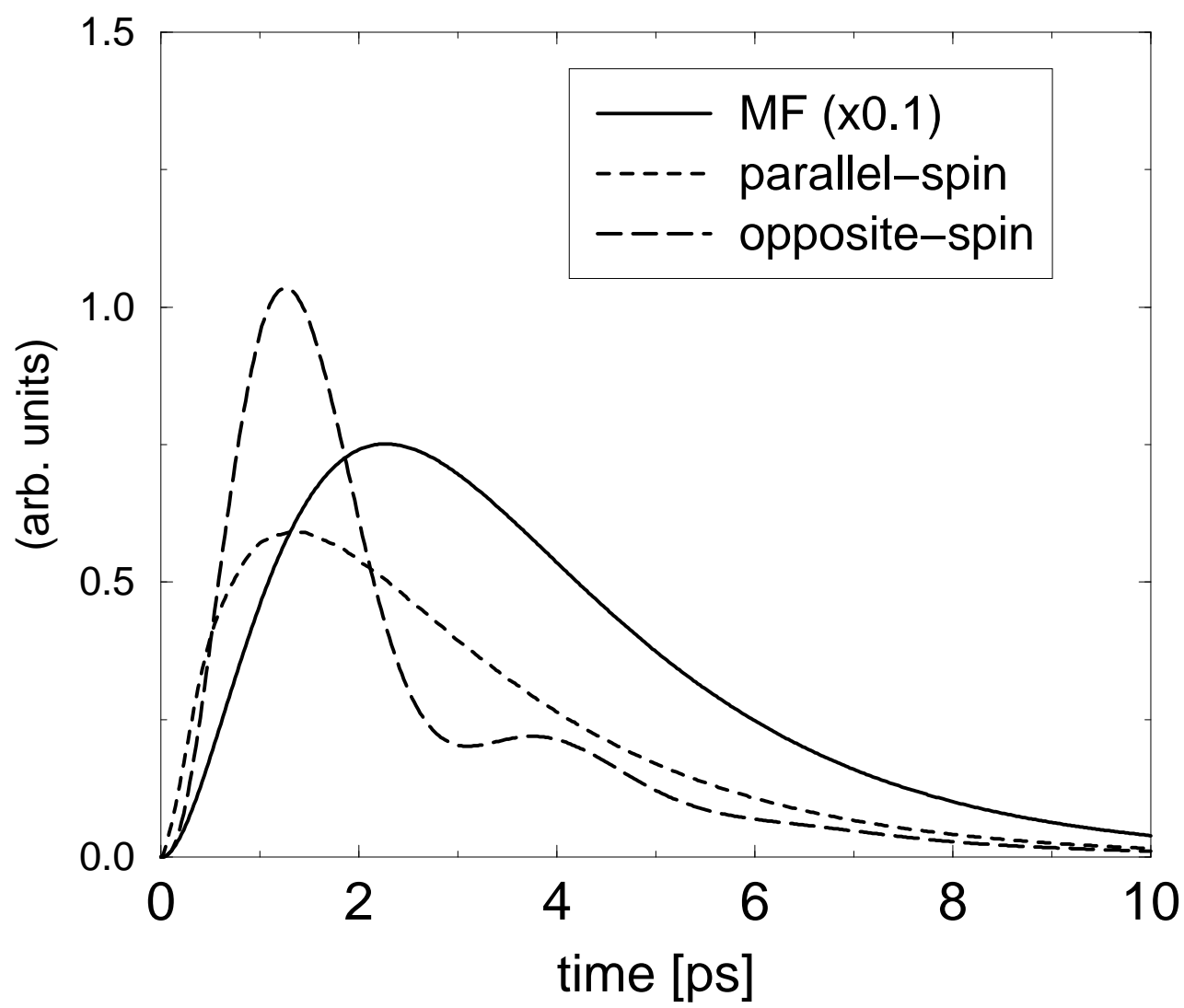
oestreich et al.: theory of exciton-exciton ...

Figure 3

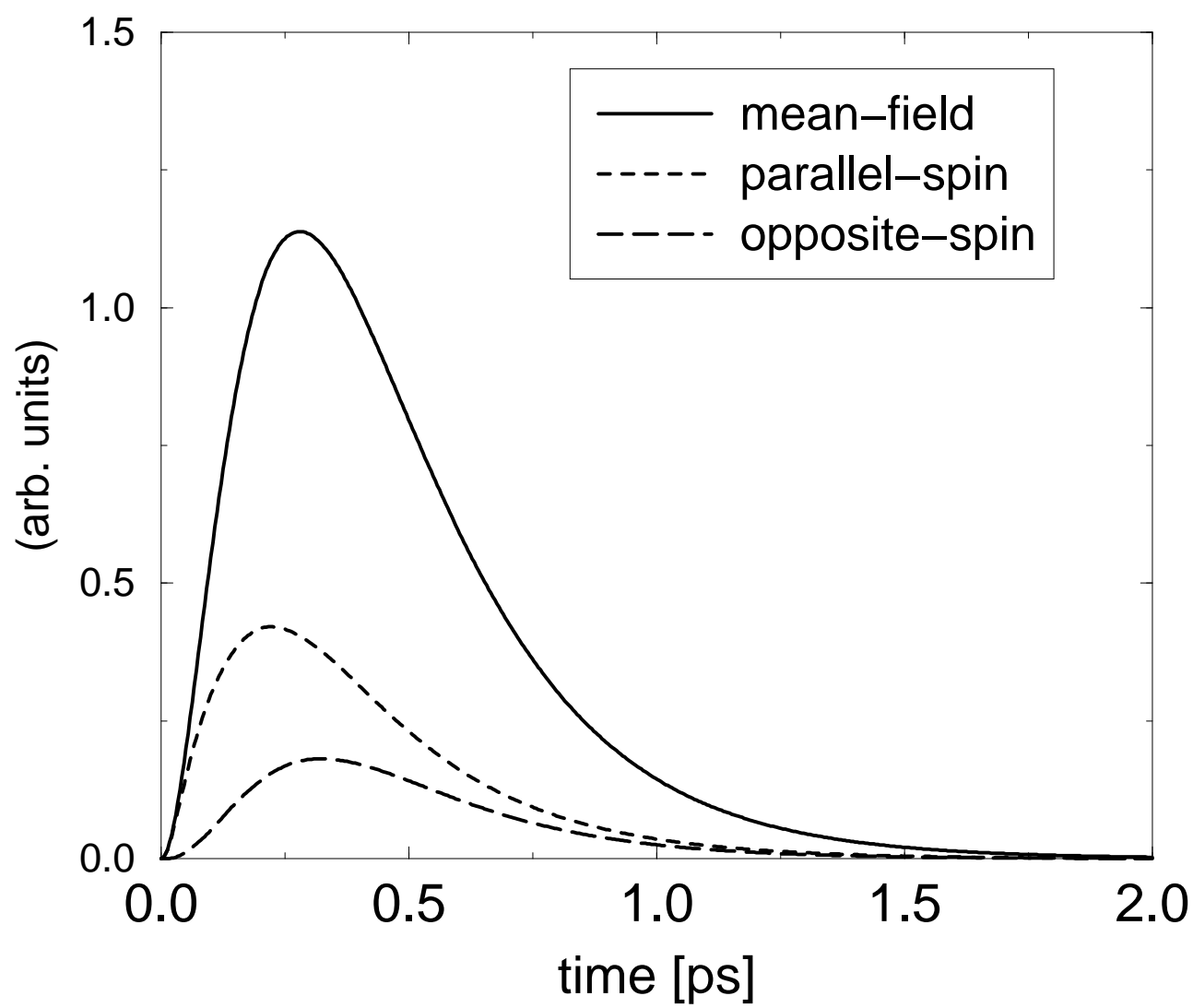


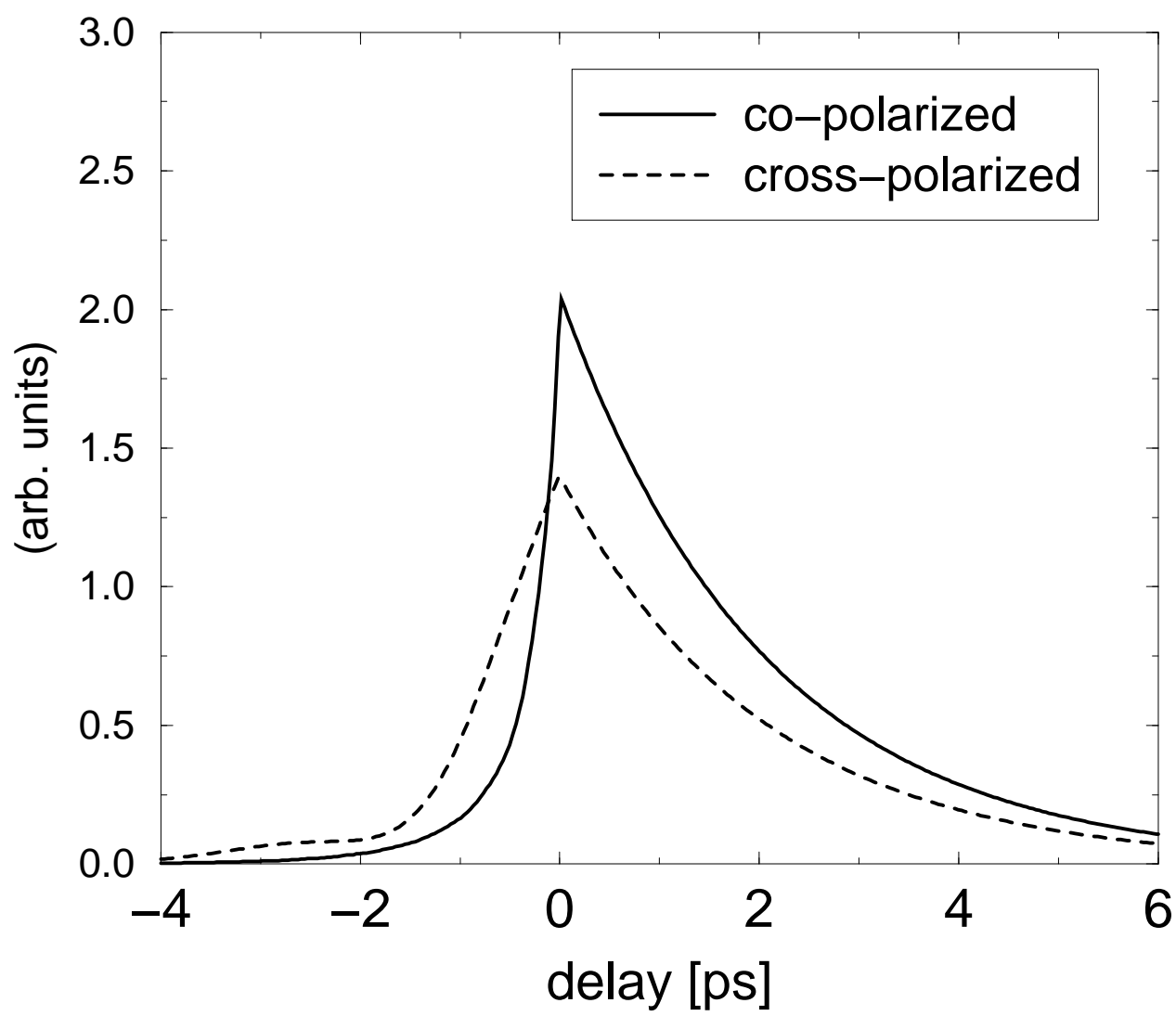






oestreich et al.: theory of exciton-exciton ... Figure 6





oestreich et al.: Theory of exciton-exciton ... Figure 8

